Volterra Systems with Realizable Kernels

Hoan Kim Huynh Nguyen

Dissertation submitted to the Faculty of the
Virginia Polytechnic Institute and State University
in partial fulfillment of the requirements for the degree of

Doctor of Philosophy
in
Mathematics

Terry L. Herdman, Chair
Jeff T. Borggaard
John A. Burns
Eugene M. Cliff
Belinda B. King
Robert C. Rogers

Date: April 28, 2004
Blacksburg, Virginia

Keywords: Realization Theory, Delay Equations, Internal State, Volterra Integro-Differential Equations, Runge-Kutta Method.

Volterra Systems with Realizable Kernels

Hoan Kim Huynh Nguyen

(ABSTRACT)

We compare an internal state method and a direct Runge-Kutta method for solving Volterra integro-differential equations and Volterra delay differential equations. The internal state method requires the kernel of the Volterra integral to be realizable as an impulse response function. We discover that when applicable, the internal state method is orders of magnitude more efficient than the direct numerical method. However, constructing state representation for realizable kernels can be challenging at times; therefore, we propose a rational approximation approach to avoid the problem. That is, we approximate the transfer function by a rational function, construct the corresponding linear system, and then approximate the Volterra integro-differential equation. We show that our method is convergent for the case where the kernel is nuclear. We focus our attention on time-invariant realizations but the case where the state representation of the kernel is a time-variant linear system is briefly discussed.

This research is supported in partly by the Air Force Office of Scientific Research under Grant F49620-C-0048 and Grant F49620-00-1-0299.

To my parents and brother,
with love.

Acknowledgements

First and foremost, I would like to thank my advisor, Dr. Herdman, for his constant encouragement and endless support, especially this past year. Dr. Herdman has not only taught me math in the classroom, given me directions on my research, and opened my eyes to opportunities, he has also given me guidance in handling other situations in life. I feel very fortunate to be one of his students. Dr. Herdman, I will definitely miss integrating those integrals with you and I cannot tell you how much I appreciate everything you have done for me!!

I am also indebted to Professor Burns for this awesome research topic and his scientific research advice. Dr. Burns is always willing to talk even late in the evening.

I would also like to express my gratitude to Professor Cliff for always willing to discuss my problems, answer my many questions, and clear up all of my confusions. Dr. Cliff has also helped me with my codes and also letting me use his codes on the average and linear spline schemes.

Dr. Borggaard - I will never forget you telling me to plant the seed for graduate school when I left to go to NRL.

Dr. Gao - thank you for introducing me to research as an undergraduate and encouraging me to go to graduate school.

I would also like to thank Dr. King and Dr. Rogers for their support and patience during my graduate career.

I would like to thank everyone in the math department. All of the teachers I have had in the math department from whom I have gained all my mathematical knowledge; those who I have worked with, who made work very enjoyable; and to the staff-thank you for all the help, from computers to paperwork. Everyone has been so wonderful and helpful since my first day at Tech.

To my family and friends-thank you for your encouragement and support for many years. Especially to those friends I have met at Tech-thank you for making Tech feel like home for the whole time I have been here. John Singler-thank you for letting me use your finite elements codes, and Lisa-thank you for editing my dissertation.

Last but definitely not least, I would like to express my greatest gratitude to my parents and my brother for their endless love, encouragement, and support throughout the years. Mom and Dad, thank you for your sacrifices to bring me to this land of opportunity and for helping to make my dreams come true. Mom, thank you for always being there to listen and believe in me even at the lowest points in my life. Dad, words cant express how much I admire your intuition in life and appreciate your sacrifices so that I can be who I am today. Thank you for all of your advice and guidance in life; they have always amazed me. To my younger but not so little brother, Vu, thank you for all of the laughter you have brought to my life, I am very proud of you.

Contents

List of Figures

List of Tables

Chapter 1

Introduction

1.1 Volterra Integral Equations

Volterra equations are used in many applied sciences to model dynamical systems. They have been seen in aero-elastic systems [13], viscoelastic and electromagnetic materials [3 and 7], and biological systems [2 and 23], just to name a few. A great deal of work has been done on both the theoretical and numerical aspects of Volterra equations for many decades. We are especially interested in the numerical methods used to solve Volterra integro-differential equations and Volterra delay differential equations.

A Volterra integral equation is a functional equation in which the unknown function appears under at least one integral sign and the upper limit of integration is a variable. If the equation contains a derivative of this unknown function, we call the equation a Volterra integro-differential equation. Let $I := [0, T]$ be a given closed and bounded interval with $0 < T$, and $S := \{(t, s) : 0 \leq s \leq t \leq T\}$. An integral equation (for the unknown function x)

$$x(t) = f(t, x(t)) + \int_0^t k(t, s)x(s)ds, \qquad t \in I, \tag{1.1}$$

is called a nonlinear Volterra integral equation of the second kind. Here, f and k are given real-valued functions where k is the kernel of the equation, and f is sometimes referred to as the forcing function, or as the initial function.

In integral equations of the first kind, the unknown function occurs only under the integral sign. Hence, a linear Volterra integral equation of the first

kind is written as

$$f(t) = \int_0^t k(t,s)x(s)ds, \qquad t \in I. \tag{1.2}$$

Let $\theta(t)$ be a continuous function possessing a finite number of zeros in the interval I. A Volterra integral equation of the third kind

$$\theta(t)x(t) = f(t,x(t)) + \int_0^t k(t,s)x(s)ds, \qquad t \in I, \tag{1.3}$$

may be viewed as the generalization of the second kind integral equation.

In this research, we focus on the special nonlinear case of first order nonlinear Volterra integro-differential equations where the nonlinearity is in the forcing function f but the integrand is linear and of convolution type in $x(s)$

$$\begin{aligned} \dot{x}(t) &= f(t,x(t)) + \int_0^t K(t-s)x(s)ds, \\ x(0) &= \eta \in \mathbb{R} \end{aligned} \tag{1.4}$$

where $f : \mathbb{R}^2 \to \mathbb{R}$, $x : \mathbb{R} \to \mathbb{R}$, and $K : \mathbb{R} \to \mathbb{R}$.

Another class of Volterra equations that we are interested in is the Volterra delay differential equations of the form

$$\begin{aligned} \dot{x}(t) &= f(t,x(t)) + x(t-r) + \int_0^t K(t-s)x(s)ds, \\ x(\tau) &= \varphi(\tau), \qquad \tau \in [-r,0) \\ x(0) &= \eta \in \mathbb{R} \end{aligned} \tag{1.5}$$

where $r > 0$, $f : \mathbb{R}^2 \to \mathbb{R}$, $x : \mathbb{R} \to \mathbb{R}$, $K : \mathbb{R} \to \mathbb{R}$, and $\varphi \in L_2[-r,0)$.

1.2 Realization Theory

Realizability is the study of the construction of state representations from a given input-output description *weighting pattern* (or the transform of a *weighting pattern* called a *transfer function*). That is, given a *weighting pattern* $K(t) \in L(\mathbb{R}^m \to \mathbb{R}^p)$ defined by

$$y(t) = \int_0^t K(t-s)u(s)ds$$

(or a *transfer function* $\hat{K}(s)$), we would like to know when a system

$$\begin{aligned} \dot{z}(t) &= Az(t) + Bx(t) \\ y(t) &= Cz(t) \\ z(0) &= 0, \end{aligned} \tag{1.6}$$

can be constructed such that $K(t)$ has the representation of $K(t) = Ce^{At}B$. Here $A : X \to X$, $B : U \to X$, and $C : X \to Y$ where X, U, Y are the state, input, and output spaces respectively. Mathematicians have spent at least the past fifty years studying the relation between transfer functions and models that realize them. A great deal of work has been done in both finite dimensional realization and infinite-dimensional realization with discrete and continuous time. This research focuses on the relationship of transfer functions and their realized linear systems in finite and infinite dimensional spaces with continuous time.

In the finite dimensional case, we consider a continuous-real valued function $K(t)$ defined on $[0, \infty)$ that is an impulse response function. Then we attempt to construct $A \in L(\mathbb{R}^n, \mathbb{R}^n)$, $B \in L(\mathbb{R} \to \mathbb{R}^n)$, and $C \in L(\mathbb{R}^n \to \mathbb{R})$ such that $K(t) = Ce^{At}B$. The function $K(t)$ is said to be realizable if and only if it can be written as $K(t) = Ce^{At}B$. Given $K(t)$, we can find its transfer function, $\hat{K}(s)$, by taking the Laplace transform of $K(t)$. The Laplace transform we consider in this manuscript is the unilateral Laplace transform defined by the integral

$$\hat{K}(s) = \int_{0^+}^{\infty} K(t)e^{-st}\, dt$$

for all values of s for which the integral exists (converges) [24]. Once we have a transfer function, $\hat{K}(s)$, we can construct infinitely many state representations of $\hat{K}(s)$. However, there exists only one minimal realization for each transfer function upto coordinate changes (bases) in the state space [22]. One thing to notice is that in the finite dimensional case, the realizations we construct from $K(t)$ are always systems of ODE.

In the infinite dimensional case, similarly, $K(t)$ is said to be realizable if and only if it can be written as $K(t) = Ce^{At}B$. Here, for an unbounded operator A, we will use e^{At} to denote the associated semigroup. We will consider the results in the infinite dimensional case in two separate circumstances. First, we will discuss results from Baras and Brocket [11] where B and C are required to be bounded. However, when B and C are chosen to

be conveniently bounded, most standard applications are eliminated. For instance, examples of loss-less transmission lines discussed in [21] where B is a distribution and C is an unbounded operator are ignored by Baras and Brokett. Helton [21] extended Baras and Brockett's results to a more general case where B and C can be unbounded. Here, we will state and discuss the main results; the detailed proof of these results can be found in [11] and [21].

Baras and Brocket work with the most basic Hilbert space, $l_2(\mathbb{Z}^+) = \{\{a_i\}, i = 1, 2, 3, ...,$ such that $\{a_i\}$ is a square summable sequence$\}$. If A is a bounded operator on $l_2(\mathbb{Z}^+)$, B is a bounded operator on $l_2(\mathbb{Z}^+)$, and C is a bounded linear functional on $l_2(\mathbb{Z}^+)$, then we call $[A, B, C]$ a *bounded realization*. $[A, B, C]$ is called a *regular realization* if A is instead the infinitesimal generator of a strongly continous semigroup of bounded operators e^{At} on $l_2(\mathbb{Z}^+)$. For the cases where A is the infinitesimal generator of a strongly continous semigroup of bounded operators e^{At} on $l_2(\mathbb{Z}^+)$, B is restricted to be in the domain of A (written as $D_0(A)$), and C is a linear functional defined on $D_0(A)$ with $|C(u)| \leq \beta(||Au|| + ||u||)$ for all $u \in D_0(A)$ and some constant β, we call such realizations *balanced realizations*. We provide the following definitions and results that we will employ in this paper.

Definition 1.1 *(Baras and Brockett [11]) A weighting pattern $K(t)$ is realizable if and only if it has a balanced realization.*

□

Theorem 1.1 *(Baras and Brockett [11]) A weighting pattern $K(t)$ has a balanced realization if and only if it has a regular one.*

□

Theorem 1.2 *(Baras and Brockett [11]) A necessary condition for $K(t)$ to be realizable is that it is continuous and of exponential order (i.e., ess $\sup |K(t)| \leq M_0 e^{\gamma t}$ for some positive M_0, γ). A sufficient condition is that $K(t)$ is locally absolutely continuous (i.e., absolutely continuous, on each bounded closed interval) and that $\dot{K}(t)$ (which then exists as an a.e. defined function) be of exponential order (i.e., ess $\sup |\dot{K}(t)| \leq M e^{\alpha t}$ for some positive M, α).*

□

Let Π_ρ^+ denotes the right half plane where Re $s > \rho$ and $H^2(\Pi_\rho^+)$ denotes the space of functions which are analytic in Π_ρ^+ and square integrable along vertical lines in Π_ρ^+ such that

$$\sup_{u>\rho} \int_{-\infty}^{\infty} |f(u+iw)|^2 \, dw \leq M < \infty.$$

We will be consistent with the literature using the notations given above.

Theorem 1.3 *(Baras and Brockett [11]) A necessary condition for $K(t)$ to be realizable is that its Laplace transform $\hat{K}(s)$ belongs to $H^2(\Pi_\rho^+) \bigcap H^\infty(\Pi_\rho^+)$ for some $\rho > 0$. A sufficient condition is that $\hat{K}(s) \in H^2(\Pi_\rho^+)$ and $(s\hat{K}(s) - K(0)) \in H^2(\Pi_\rho^+)$ for some $\rho > 0$.*

□

As a consequence of Theorem 1.3, $\hat{K}(s) = \frac{e^{-s}}{s^2}$ is realizable but $\hat{K}(s) = \frac{e^{-s}}{s}$ is not realizable [11]. These examples of transfer functions will be discussed more in the examples later. Baras and Brockett constructed A to be a differentiation operator on $L_2(0,\infty)$. The domain of A is defined to be $D_0(A) = \{f \in L_2(0,\infty) | \, f$ is locally absolutely continous; $f' \in L_2(0,\infty)\}$. B is defined to be a map from $L_2(0,\infty)$ to $D_0(A)$ and C is a linear functional on $D_0(A)$. Before we move on to Helton's theorem, we use $L(H_1, H_2)$ to denote the space of all bounded linear operators with the norm

$$||A|| = \max_{u \in H_1} \frac{||Au||_{H_2}}{||u||_{H_1}}$$

where H_1 and H_2 are Hilbert spaces.

Definition 1.2 *(Helton [21]) Let A be an infinitesimal generator of a strongly continuous semigroup of bounded operators e^{At}, $B : U \rightarrow D_0(A^*)'$ and $C : D_0(C) \rightarrow Y$. Here $D_0(A^*)'$ is the dual of $D_0(A^*)$, A^* is the adjoint of A, and $D_0(A) \subset D_0(C) \subset D_0(A^*)'$.*

(a) A system $[A, B, C]$ is a compatible system if it satisfies $(\lambda I - A)^{-1}B \subset D_0(C)$ for some λ with Re $\lambda > 0$.

(b) The controllability map $\mathcal{C} : L^1(U) \to D_0(A^*)'$ *is*

$$\mathcal{C}\,\mathbf{u} = \int_0^\infty e^{At} B\, u(t)\, dt$$

where $\mathbf{u}$ *is the function* $u(t)$ *in* $L^1(U)$.

(c) The observability map $\mathcal{Q} : L^1(Y) \to D_0(A)$ *is*

$$\mathcal{Q}\,\mathbf{y} = \int_0^\infty [Ce^{At}]^*\, y(t)\, dt.$$

(d) The frequency-response function (FRF) is

$$C(\lambda I - A)^{-1} B$$

for Re $\lambda > 0$.

□

Theorem 1.4 *(Helton [21]) If* $\hat{K}(s)$ *is a uniformly bounded* $L(U, Y)$*-valued analytic function on the right half plane (RHP) with a limit* $\hat{K}(\infty)$ *in the positive direction, then there is a compatible continuously controllable and observable system satisfying* $||e^{At}|| \leq 1$ *with* $\hat{K}(s)$ *as its frequency-response function.*

□

Helton also constructed the operator A to be a differentiation operator but on the domain $D_H = \{f \in L_2(-\infty, \infty) | f' \text{ is in } L_2(0, \infty)\}$, $B : U \to D_H(A)$ and $C : D_H(A) \to Y$. Helton's result confirms the existence of the state representation for a more general class of kernel. In particular, it guarantees realizations that allow us to apply our internal state method. In Chapter 2, we show the connection between realization theory and this internal state numerical method. Throughout this dissertation, we will refer to the class of kernels that is realizable by Theorem 1.3 as bounded-realizable kernels and the class of kernels that is realizable by Theorem 1.4 as realizable.

1.3 Overview

The major contributions of this study are the comparison of computing time between different numerical methods and the construction of realization for a large classes of kernels. In addition, we also contribute theoretical results on convergence of rational approximation method for nuclear kernels.

The focus of this dissertation is on numerical approximations for a class of Volterra equations. The two numerical methods we study are an internal state method and a direct numerical method. We present and discuss in Section 2.1 the internal state method in both the finite and the infinite dimensional cases. Also, the direct numerical method is presented in Section 2.2. Chapter 3 illustrates and discusses possible issues with these two methods using a variety of applications. In Chapter 4, we show convergence of approximate solutions to Volterra integro-differential equations for the case where $K(t)$ is of nuclear type. Chapter 5 presents conclusions and future direction for this research.

Chapter 2

Numerical Methodology

2.1 Internal State Method

The internal state method has been frequently employed by researchers for several years. It is similar to the *internal variables* idea employed in mechanics [1 and 9] and aeroelasticity [13]. See also [6] and [7] for discussions of the relationship between internal variable models, Boltzmann hysteresis and Volterra operator formulations in viscoelastic materials. References [8] and [19] contain applications to biotissues.

The idea of the internal state method is to rewrite the Volterra equation such that the integral is a component of the solution of the constructed system. This idea goes hand in hand with realization theory in which the kernel $K(t)$ of the Volterra equations is the function that we want to realize. In fact, the internal state method is only applicable if the kernel $K(t)$ is realizable.

2.1.1 Finite Dimensional Case

Consider a nonlinear Volterra integro-differential equation

$$\begin{aligned} \dot{x}(t) &= f(t, x(t)) + \int_0^t K(t-s)x(s)ds, \\ x(0) &= \eta \in \mathbb{R} \end{aligned} \tag{2.1}$$

where $f : \mathbb{R}^2 \to \mathbb{R}$, $x : \mathbb{R} \to \mathbb{R}$, and $K : \mathbb{R} \to \mathbb{R}$. If the given $K(t)$ is continuous and represents an impulse response function (i.e., the response

at time t to an input $x(\cdot)$ is defined by $\int_{-\infty}^{\infty} K(t,\tau)u(\tau)\,d\tau)$, we can use realization theory for finite dimensional systems to construct $A \in L(\mathbb{R}^n, \mathbb{R}^n)$, $C \in L(\mathbb{R}^n \to \mathbb{R})$, and $B \in L(\mathbb{R} \to \mathbb{R}^n)$ so that $K(t) = Ce^{At}B$. Note that $n \in \mathbb{Z}^+$ is not given but to be determined from $K(t)$. It follows that $\int_0^t K(t-s)x(s)\,ds$ is the solution of the following system

$$\begin{aligned} \dot{z}(t) &= Az(t) + Bx(t), \\ y(t) &= Cz(t), \\ z(0) &= 0. \end{aligned} \tag{2.2}$$

Thus, the Volterra integro-differential equation (2.1) can be represented as

$$\begin{aligned} \dot{x}(t) &= f(t, x(t)) + y(t), \\ \dot{z}(t) &= Az(t) + Bx(t), \\ y(t) &= Cz(t), \\ x(0) &= \eta, \\ z(0) &= 0. \end{aligned} \tag{2.3}$$

Similarly, the Volterra delay differential equation

$$\begin{aligned} \dot{x}(t) &= f(t, x(t)) + x(t-r) + \int_0^t K(t-s)x(s)\,ds, \\ x(\tau) &= \varphi(\tau), \qquad \tau \in [-r, 0], \\ x(0) &= \eta \in \mathbb{R}, \end{aligned} \tag{2.4}$$

where $f : \mathbb{R}^2 \to \mathbb{R}$, $x : \mathbb{R} \to \mathbb{R}$, $K : \mathbb{R} \to \mathbb{R}$, and $\varphi \in L_2[-r, 0)$ for $r > 0$, can be represented as:

$$\begin{aligned} \dot{x}(t) &= f(t, x(t)) + x(t-r) + y(t), \\ \dot{z}(t) &= Az(t) + Bx(t), \\ y(t) &= Cz(t), \\ x(0) &= \eta, \\ z(0) &= 0, \\ x(\tau) &= \varphi(\tau), \qquad \tau \in [-r, 0]. \end{aligned} \tag{2.5}$$

where A, B, C and their dimensions are determined by K.

Numerical solutions of the linear system (2.3) constructed from the internal state method are computed by a Runge-Kutta method of order four

and the constructed delay system (2.5) is also computed by a fourth order Runge-Kutta method with the method of steps (see [18]) unless stated otherwise.

2.1.2 Infinite Dimensional Case

In the infinite dimensional case, we will only consider Volterra integro-differential equations since we want to illustrate the infinite dimensional state representations of kernels that include delay systems.

Consider a Volterra system

$$\begin{aligned} \dot{x}(t) &= f(t, x(t)) + \int_0^t K(t-s)x(s)ds, \\ x(0) &= \eta \in \mathbb{R} \end{aligned} \tag{2.6}$$

where $f : \mathbb{R}^2 \to \mathbb{R}$, $x : \mathbb{R} \to \mathbb{R}$, and $K : \mathbb{R} \to \mathbb{R}$. If the Laplace transform $\hat{K}(s)$ of $K(t)$ is such that $\hat{K}(s) \in H^2(\Pi_\rho^+)$ and $(s\hat{K}(s) - K(0)) \in H^2(\Pi_\rho^+)$ for some $\rho > 0$, then by Theorem 1.3 and the definition of realizable, the Volterra system (2.6) above can be represented as

$$\begin{aligned} \dot{x}(t) &= f(t, x(t)) + Cz(t) \\ \dot{z}(t) &= Az(t) + Bx(t) \\ x(0) &= \eta \in \mathbb{R} \\ z(0) &= 0, \end{aligned} \tag{2.7}$$

where A is a closed operator on $L_2(0, \infty)$ with a dense domain in a Banach space X which also generates a C_0 semigroup; $B : \mathbb{R} \to D_0(A)$ and $C : D_0(A) \to \mathbb{R}$ are bounded. However, in a more general case, if $\hat{K}(s)$ is a uniformly bounded $L(\mathbb{R}, \mathbb{R})$-valued analytic function on an open right half plane (RHP) with a limit $\hat{K}(\infty)$ in the positive direction, then it follows from Helton's result above that the Volterra system (2.6) can also be written as a linear system (2.7). Helton defined the operator A on the space $L_2(-\infty, \infty)$ with B, C unbounded. Allowing B and C to be unbounded, we can realize a larger class of kernel that covered by the theory in Baras and Brockett. Once contructed, linear system (2.7) is normally approximated by a fourth order Runge-Kutta method unless stated otherwise.

2.2 Direct Numerical Method

Direct numerical methods for solving Volterra equations and Volterra integro-differential equations are discussed in detail by Brunner and van der Houwen [12]. They have studied numerous numerical schemes and quadatures for solving Volterra equations. In addition to providing details of each numerical scheme, Brunner and van der Houwen also discuss stability and convergence rate of each method. Our direct numerical method for solving the Volterra integro-differential equation (2.1) or (2.6) is Brunner and van der Houwen's Runge-Kutta method. We provide an overview of the results regarding numerical solution for Volterra equations.

Consider the Volterra integro-differential equation (VIDE) of the form:

$$\begin{aligned} \dot{x}(t) &= f(t, x(t), z(t)), \qquad t \in I = [0, T] \\ x(0) &= x_0 \in \mathbb{R}, \end{aligned}$$

where,

$$z(t) = \int_0^t k(t, s, x(s))\, ds.$$

After the interval $[0, T]$ is discretized by a uniform mesh $\{t_n\}$, (VIDE) can be put in the form:

$$\begin{aligned} \dot{x}(t) &= f\left(t, x(t), F_n(t) + \int_{t_n}^t k(t, s, x(s))\, ds\right), \qquad t \in [t_n, T] \\ x(0) &= x_0, \end{aligned}$$

where the lag term, $F_n(t)$, is defined as:

$$F_n(t) = \int_0^{t_n} k(t, s, x(s))\, ds, \qquad n = 0, ...N - 1.$$

At $t = t_{n+1} = t_n + h$, the (VIDE) will be discretized by:

$$x_{n+1} = x_n + h \sum_{j=1}^{m} b_j f(t_n + c_j h, X_{n,j}, \hat{F}_n(t_n + c_j h) + h\hat{\phi}_n(t_n + c_j h)),$$

$$n = 0, ..., N - 1,$$

with the given initial value $x_0 = x(0)$, and $X_{n,j}$, $\hat{\phi}_n$, and $\hat{F}_n$ are defined below.

Definition 2.1 *(a) An m-stage VIDE-Runge-Kutta formula (VDRK formula) for (VIDE) has the form*

$$X_{n,j} = x_n + h\sum_{i=1}^{m} a_{j,i} f(t_n + c_i h, X_{n,i}, \hat{F}_n(t_n + c_i h) + h\hat{\phi}_n(t_n + c_i h)),$$

$$j = 1, ..., m,$$

with $x_0 = x(0)$*;*

$$\hat{\phi}_n(t_n + c_i h) = \sum_{l=1}^{m} \bar{a}_{i,l} k(t_n + d_{i,l}h, t_n + c_l h, X_{n,l}), \qquad i = 1, ..., m.$$

(b) the VDRK method is called an extended VDRK method if the lag term formula is given by

$$\hat{F}_n(t) := h\sum_{l=0}^{n-1}\sum_{j=1}^{m} b_j k(t, t_l + c_j h, X_{l,j}), \qquad n = 1, ..., N-1.$$

□

Here the vectors $\mathbf{c} := (c_j)$, $\mathbf{b} := (b_j)$ and the square matrices $\mathbf{A} := (a_{j,i})$, $\bar{\mathbf{A}} := (\bar{a}_{i,l})$, $\mathbf{D} := (d_{i,l})$ are given. Also, we employ the notation

$$Z_{n,i} := \hat{\phi}_n(t_n + c_i h)$$

to be consistent with Brunner and van der Houwen [12].

Definition 2.2 *A VDRK method (or a VDRK formula) is said to be explicit if* $a_{j,i} = 0$, $1 \le j \le i \le m$, *and* $\bar{a}_{i,l} = 0$, $1 \le i < l \le m$ *(i.e., if the matrices* $\mathbf{A}$ *and* $\bar{\mathbf{A}}$ *are, respectively, of strictly lower triangular and of lower triangular form).*

□

Definition 2.3 *A Volterra integro-differential equation (VIDE)-Runge-Kutta formula is said to be of Bel'tyukov type (a BVDRK formula) if*

$$d_{i,l} = d_l, \qquad i, l = 1, ..., m.$$

It satisfies the kernel condition if

$$d_l \ge c_l$$

holds whenever $\bar{a}_{i,l} \ne 0$*. A BVDRK formula is characterized by the diagram*

$\mathbf{d}$	$\bar{\mathbf{A}}$	$\mathbf{c}$	$\mathbf{A}$
			$\mathbf{b^T}$

□

The diagram in Definition 2.3 represents the coefficients in the VDRK formulas in Definition 2.1. The diagram also denotes that vectors $\mathbf{d}$, $\mathbf{c}$ have the same number of rows as matrix $\mathbf{A}$ and $\mathbf{b^T}$ has the same number of columns as matrix $\mathbf{A}$. Also, matrix $\mathbf{A}$ and its conjugate, $\bar{\mathbf{A}}$, are square matrices. Definitions 2.1, 2.2, and 2.3 correspond to Definition 4.2.1, 4.2.2 (i), and 4.2.4 in [12], respectively. Moreover, a BVDRK satisfies the *kernel condition* if all points (t, s) at which the kernel has to be evaluated lie in $S = \{(t, s) : 0 \leq s \leq t \leq T\}$. Theorem 2.1 and 2.2 below are, respectively, Theorem 1.3.10 and Theorem 4.2.4 in [12].

Theorem 2.1 *For the equation $\dot{x}(t) = f(t, x(t), z(t))$, with $z(t) = \int_0^t k(t, s, x(s))ds$, $t \in I$, suppose that $f(t, x, z)$ and $k(t, s, x)$ are, respectively, continuous for $t \in I = [0, T]$ and $(t, s) \in S$, and let the following (uniform) Lipschitz conditions hold:*

$$\begin{aligned} (i) \qquad |f(t, x_1, z) - f(t, x_2, z)| &\leq L_1|x_1 - x_2|, \\ (ii) \qquad |f(t, x, z_1) - f(t, x, z_2)| &\leq L_2|z_1 - z_2|, \\ (iii) \qquad |k(t, s, x_1) - k(t, s, x_2)| &\leq L_3|x_1 - x_2|, \end{aligned}$$

for all $t \in I$, $(t, s) \in S$, $L_i \in \mathbb{R}$, and $|x_i| < \infty$, $|z_i| < \infty \quad (i = 1, 2)$.
Then for each x_0 there exists exactly one solution $x \in C^1(I)$ of (VIDE) satisfying $x(0) = x_0$.

□

Theorem 2.2 *Let the VDRK formula in Definition 2.1(a) be consistent of (local) order p, and let $\hat{F}_n(t)$ be the extended lag term formula (Definition 2.1(b)). Moreover, assume that the functions $f(t, x, s)$ and $k(t, s, x)$ characterizing the VIDE satisfy the hypotheses of Theorem 2.1 and are such that the corresponding solution $x(t)$ is sufficiently smooth on I. Then the approximations x_n generated by the extended VDRK method (Definition 2.1) are convergent of order p; i.e., we have, for $x_0 = x(0)$,*

$$\max_{1 \leq n \leq N} |x(t_n) - x_n| \leq Ch^p \qquad (\text{as } h \downarrow 0, \text{with } Nh = T),$$

where the constant C is independent of N and h.

□

For the Volterra delay differential equation (2.4), we employ a modification of Brunner and van der Houwen's formulas based on the method of steps, [see 18]. Let $k(t,s,x(s)) = K(t,s)x(s)$ and, since $x(t-r)$ is a known function of t for $t \in [jr,(j+1)r]$, when we wish to approximate the solution on $[jr,(j+1)r]$, we can write the Volterra delay differential system (2.4) in a general form such as

$$\begin{aligned} \dot{x}(t) &= f(t,x(t),z(t)), \qquad t \in [0,T] \\ x(0) &= \eta, \end{aligned} \tag{2.8}$$

where

$$z(t) = \int_0^t k(t,s,x(s))\,ds.$$

Discretize the interval $[0,T]$ by a uniform mesh, and represent (2.8) by

$$\begin{aligned} \dot{x}(t) &= f(t,x(t),F_n(t) + \int_{t_n}^t k(t,s,x(s))\,ds), \qquad t \in [t_n,T] \\ x(0) &= \eta, \end{aligned} \tag{2.9}$$

where the lag term, $F_n(t)$, is defined as

$$F_n(t) = \int_0^{t_n} k(t,s,x(s))\,ds, \qquad n = 0,...N-1. \tag{2.10}$$

Equivalently,

$$F_n(t) = \int_0^b k(t,s,x(s))\,ds + \int_b^{t_n} k(t,s,x(s))\,ds, \qquad n = 0,...N-1 \tag{2.11}$$

where $b = jr$, $j \in \mathbb{Z}^+$ (is a multiple of the time delay).

It is important in Volterra delay differential equations to write $F_n(t)$ as (2.11) instead of (2.10) because when solving for $t > b$, $x(s)$ is known for $s \in [0,b]$. The existence of the formulas in Definition 2.1 with $m = 4$ is guaranteed by Theorem 2.3 below (Theorem 4.2.3 in [12]).

Theorem 2.3 *There exist 4-stage explicit BVDRK formulas of order p=4.*

□

Moreover, Table 2.1 is the diagram of coeffiecients in Definition 2.3 (see page 226 in [12]). With the chosen coefficients, the VDRK formulas in Definition 2.1 are of Bel'tyukov type and explicit. If the Volterra integro-differential equation in (2.1) and the Volterra delay differential equation (2.4) satisfy the hypotheses in Theorem 2.3, then Theorem 2.2 implies the extended BVDRK formulas converge with order $p = 4$. We use four-stage explicit Bel'tyukov (BVDRK) formulas of order $p = 4$ as the direct numerical method in this paper. Also, note that all the Volterra systems in this paper are linear, so the extended BVDRK formulas used converge with order $p = 4$.

d	c	A	=	$\bar{A}$		
$\frac{1}{2}$	0	0	0	0	0	
$\frac{1}{2}$	$\frac{1}{2}$	$\frac{1}{2}$	0	0	0	
1	$\frac{1}{2}$	0	$\frac{1}{2}$	0	0	
1	1	0	0	1	0	
		$\frac{1}{6}$	$\frac{1}{3}$	$\frac{1}{3}$	$\frac{1}{6}$	b^T

Table 2.1: Coefficients of Runge-Kutta formulas

Chapter 3

Numerical Results

3.1 HIV-Model

A model of the interaction between healthy cells and infected cells of HIV-1 [16] is given by:

$$\begin{aligned} \frac{dC}{dt} &= r_C C(t)\left(1 - \frac{C(t)+I(t)}{C_M}\right) - k_I C(t) I(t), \\ \frac{dI}{dt} &= k_I' \int_{-\infty}^{t} C(u) I(u) F(t-u)\, du - \mu_I I(t), \end{aligned} \tag{3.1}$$

where $C(t)$ represents the concentration of healthy cells, $I(t)$ denotes the concentration of infected cells, and $F(u)$ is the *delay kernel*. The initial functions are

$$C(s) = 0, \qquad I(s) = 0, \qquad s \in (-\infty, 0),$$

while the initial conditions are

$$C(0) = 10000/mL, \qquad I(0) = 1000/mL.$$

The parameters appearing in (3.1) are listed in Table 3.1. Culshaw et al. [16] study three special cases of $F(u)$ which yield three different models: an ODE model, a discrete time delay model, and a distributed delay model.

From the general model (3.1) above, let $F(u) = \delta(u)$. Then the system

Parameters	and Variables	Values
C_0	initial amount of healthy cells	1×10^4/mL
I_0	initial amount of infected cells	1000/mL
C_M	effective carrying capacity of healthy cells	2×10^6/mL
k_I	rate constant for cell-to-cell spread	2×10^{-6}/mL/day
r	rate constant for cell-to-cell spread	0.7/day
μ_c	death rate of healthy cells	0.02/day
μ_I	death rate of infected cells	0.3/day
r_C	$(= r - \mu c)$ effective healthy cells reproductive rate	0.68/day
k'_I	$\frac{k'_I}{k_I}$ fraction of cells surviving the incubation period	1×10^6

Table 3.1: Variables and parameters for cell-to-cell spread

in (3.1) becomes the nonlinear ODE system:

$$\begin{aligned} \frac{dC}{dt} &= r_C C(t)\left(1 - \frac{C(t)+I(t)}{C_M}\right) - k_I C(t) I(t), \\ \frac{dI}{dt} &= k'_I C(t) I(t) - \mu_I I(t), \\ C(0) &= C_0, \\ I(0) &= I_0, \end{aligned} \tag{3.2}$$

where the parameters and variables are given in Table 3.1. Now if we let $F(u) = \delta(u - \tau)$ where $\tau \geq 0$, then the general model (3.1) becomes the following delay differential equations (DDE) with a discrete delay

$$\begin{aligned} \frac{dC}{dt} &= r_C C(t)\left(1 - \frac{C(t)+I(t)}{C_M}\right) - k_I C(t) I(t), \\ \frac{dI}{dt} &= k'_I C(t-\tau) I(t-\tau) - \mu_I I(t), \\ C(0) &= C_0, \\ I(0) &= I_0, \end{aligned} \tag{3.3}$$

and the initial histories are

$$C(s) = 0, \qquad I(s) = 0, \qquad s \in [-\tau, 0).$$

Define $F(u)$ to be a *weak* kernel; that is, when $F(u) = \alpha e^{-\alpha u}$ for $\alpha > 0$, then

we have

$$\begin{aligned} \frac{dC}{dt} &= r_C C(t)\left(1-\frac{C(t)+I(t)}{C_M}\right) - k_I C(t)I(t), \\ \frac{dI}{dt} &= k_I' \int_{-\infty}^{t} C(u)I(u)\alpha e^{-\alpha(t-u)}\,du - \mu_I I(t), \\ C(0) &= C_0, \\ I(0) &= I_0, \end{aligned} \tag{3.4}$$

where the initial conditions are

$$C(s) = 0, \qquad I(s) = 0, \qquad s \in [-\infty, 0).$$

Using the internal state method, (3.4) can be written as the ODE system:

$$\begin{aligned} \frac{dC}{dt} &= r_C C(t)\left(1-\frac{C(t)+I(t)}{C_M}\right) - k_I C(t)I(t), \\ \frac{dI}{dt} &= k_I' X(t) - \mu_I I(t), \\ \frac{dX}{dt} &= \alpha C(t)I(t) - \alpha X(t), \end{aligned} \tag{3.5}$$

with the initial conditions

$$\begin{aligned} C(0) &= C_0, \\ I(0) &= I_0, \\ X(0) &= 0. \end{aligned}$$

To verify ODE system (3.5) is equivalent to Volterra system (3.4), we note that the solution of

$$\begin{aligned} \frac{dX}{dt} &= \alpha C(t)I(t) - \alpha X(t) \\ X(0) &= 0, \end{aligned}$$

by the variation of parameters formula, is

$$\int_{-\infty}^{t} C(u)I(u)\alpha e^{-\alpha(t-u)}\,du.$$

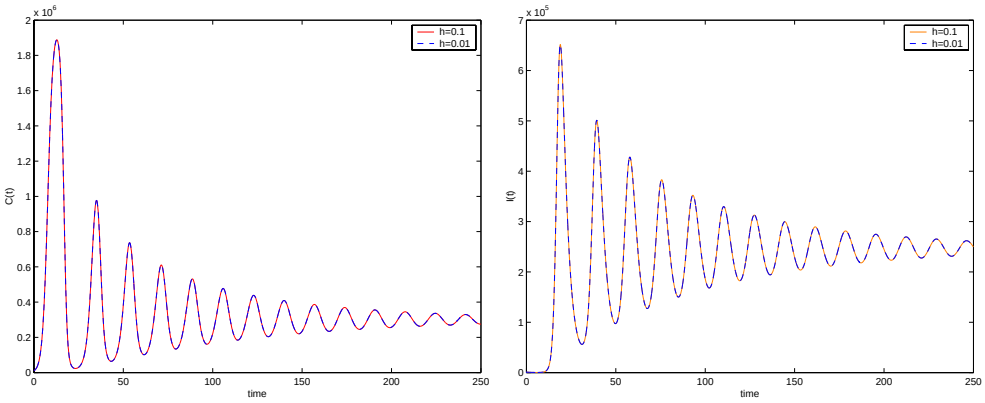

Figure 3.1: C(t) and I(t) of distributed delay model, $\alpha = 1.5$

We solve system (3.5) using a four-stage, fourth-order, explicit, fixed step Runge-Kutta method. Figure 3.1 provides the plots of $C(t)$ and $I(t)$ for $\alpha = 1.5$ using step sizes $h = 0.1$ and 0.01. MATLAB functions *ode*45 and *ode*23*s* yield identical plots. Figure 3.2 provides the solutions of (3.5) for $\alpha = 5$ using the same numerical method and the same step sizes. Also, MATLAB *ode*45 and *ode*23*s* give the same graphs as in Figure 3.2. These two simulations demonstrate that our Runge-Kutta method gives very precise approximations. Let $x(t) = (C(t), I(t))$, $x(t_n) = x_n$, and $h = \frac{1}{N}$. Define $f(t) = (f_1(t), f_2(t))$ and $z(t) = (z_1(t), z_2(t))$, where

$$\begin{aligned} f_1(t) &= r_C C(t)\left(1 - \frac{C(t) + I(t)}{C_M}\right) - k_I C(t) I(t), \\ f_2(t) &= -\mu_I I(u), \\ z_1(t) &= 0, \\ z_2(t) &= k_I' \int_0^t \alpha C(u) I(u) e^{-\alpha(t-u)}\, du. \end{aligned}$$

We next use the direct numerical method described in Section 2.2 to solve system (3.4). Figure 3.3 provides the plot of $C(t)$ and $I(t)$ using *ode*45 and the direct numerical method of step size $h = 0.01$ and $\alpha = 5$. We also solve system (3.4) using our explicit fourth order Runge-Kutta method and it provides the same graphs as in Figure 3.3. The elapsed time for solving system (3.5) using Runge-Kutta method is only 0.3310 seconds while the

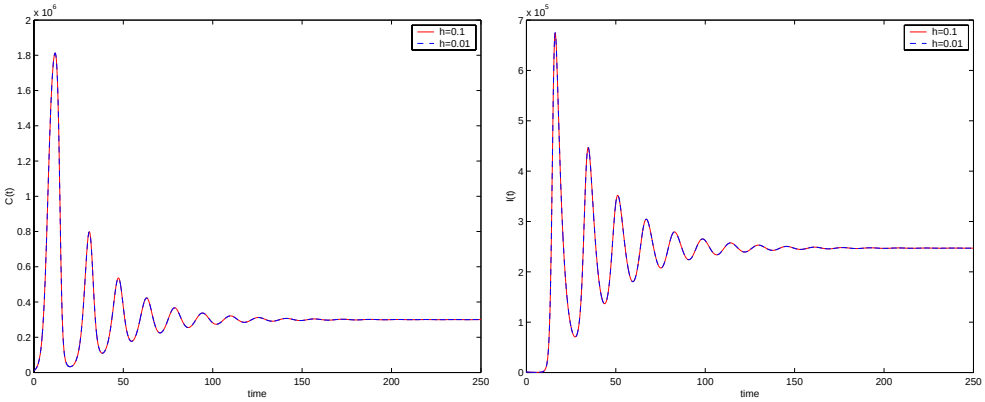

Figure 3.2: C(t) and I(t) of distributed delay model, $\alpha = 5$

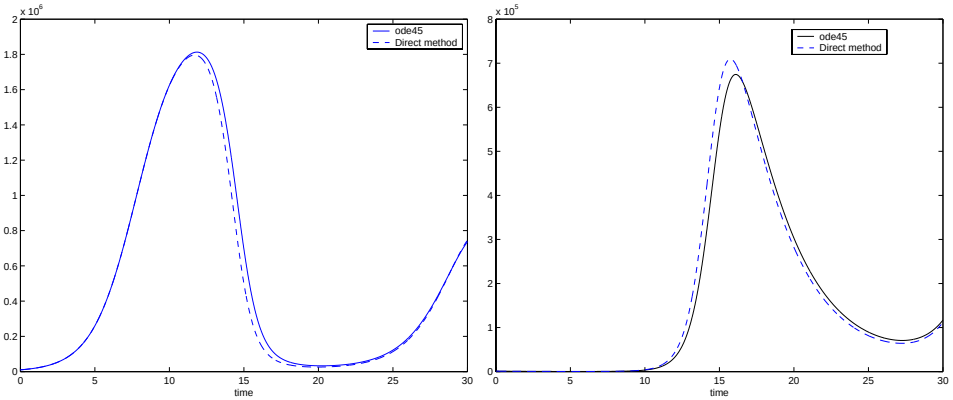

Figure 3.3: C(t) and I(t) of distributed delay model, $\alpha = 5$

elapsed time of the direct numerical method is 5.1222×10^4 seconds. It is obvious that there is a significant difference in the computing time between the internal state and the direct numerical methods. Furthermore, we restrict t to $[0, 30]$ due to the time required to compute the approximation for the direct method.

3.2 Volterra Delay Differential Equation with Exponential Kernel

This problem and the next are Volterra delay differential equations because they include time delays. The method of steps along with an explicit Runge-Kutta of fourth order are used to approximate the solutions.

Consider the Volterra delay differential equation

$$\dot{x}(t) = x(t) + x(t-1) + \int_0^t e^{3(t-s)} x(s)\, ds \qquad t > 0,$$

together with initial data

$$\begin{aligned} x(\tau) &= \frac{4}{9} - \frac{2}{3}\tau - \frac{1}{9}e^{3(\tau+1)}, \qquad \tau \in [-1, 0), \qquad (3.6) \\ x(0) &= 0. \end{aligned}$$

The exact solution of system (3.6) can be found for $t \in [0, 1]$. In fact, we construct the initial history by selecting the solution $x(t) = t$ on $[0, 1]$. That is, for $t \in (0, 1]$, we use the identity

$$1 = t + x(t-1) + \int_0^t e^{3(t-s)} s\, ds$$

to solve for $x(t-1)$, which has the representation

$$x(t-1) = \frac{4}{9} - \frac{2}{3}(t-1) - \frac{1}{9}e^{3t}.$$

Let $\tau = t - 1$; the initial function that provides the desired solution, $x(t) = t$ on $[0, 1]$, is given by

$$x(\tau) = \frac{4}{9} - \frac{2}{3}\tau - \frac{1}{9}e^{3(\tau+1)}, \qquad \tau \in [-1, 0).$$

As for the internal state method, it is known from the variation of parameter formula that

$$z(t) = e^{3t}z_0 + \int_0^t e^{3(t-s)}x(s)\,ds,$$

is the solution to the nonhomogenous linear equation

$$\dot{z}(t) = 3z(t) + x(t).$$

Thus, if we let $z(0) = z_0 = 0$, equation (3.6) can be represented as the first order delay differential equation

$$\begin{aligned} \dot{x}(t) &= x(t) + x(t-1) + z(t) \\ \dot{z}(t) &= 3z(t) + x(t), \\ x(0) &= 0 \\ z(0) &= 0, \\ x(\tau) &= \frac{4}{9} - \frac{2}{3}\tau - \frac{1}{9}e^{3(\tau+1)}, \qquad \tau \in [-1, 0). \end{aligned} \tag{3.7}$$

For the direct numerical approach, let $x(t_n) = x_n$, $h = \frac{1}{N}$ and define

$$f(t, x(t), z(t)) = x(t) + \frac{4}{9} - \frac{2}{3}(t-1) - \frac{1}{9}e^{3(t)} + z(t),$$

with

$$z(t) = \int_0^t e^{3(t-s)}x(s)\,ds, \qquad 0 < t < 1.$$

In this example, our kernel k is given by $k(t, s, x(s)) = e^{3(t-s)}x(s)$. Figure 3.4 is the plot of the exact solution along with the approximation from the internal state method and the direct numerical method. We observe that both methods are highly accurate.

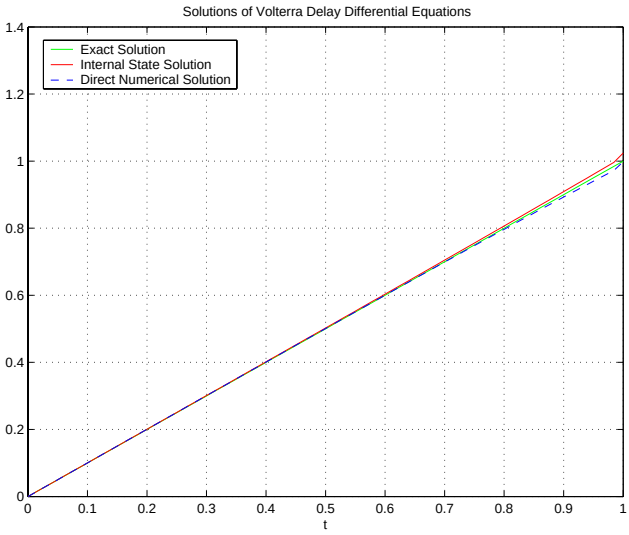

Figure 3.4: Volterra delay differential equation with exponential kernel (N = 64)

3.3 Volterra Delay Differential Equation with Cosine Kernel

Consider:

$$\begin{aligned} \dot{x}(t) &= -x(t) + x(t-1) + \int_0^t \cos(t-s)x(s)\,ds \qquad t > 0, \\ x(\tau) &= \tau, \qquad \tau \in [-1, 0), \\ x(0) &= 1. \end{aligned} \tag{3.8}$$

We seek the solution $x(t)$ on the interval [0,5]. Both numerical methods are used to construct approximating solutions. For the internal state method,

(3.8) can be written as the first order delay differential system

$$\begin{aligned} \dot{x}(t) &= -x(t) + x(t-1) + z_1(t) \\ \dot{z_1}(t) &= z_2(t) + x(t) \\ \dot{z_2}(t) &= -z_1(t), \\ x(0) &= 1 \\ z_1(0) &= 0 \\ z_2(0) &= 0, \\ x(\tau) &= \tau, \qquad \tau \in [-1, 0). \end{aligned} \tag{3.9}$$

For the direct numerical method, we define

$$f(t, x(t), z(t)) = -x(t) + (t-1) + z(t),$$

with

$$z(t) = \int_0^t \cos(t-s)x(s)\, ds.$$

Here our kernel k is given by $k(t, s, x(s)) = \cos(t-s)x(s)$. Moreover, there is a modification in the lag term formula for this example since $t \in [0, 5]$. Since $t > b = jr$, the multiple time delay $\hat{F}_n(t)$ is defined as

$$\hat{F}_n(t) = B + h\sum_{l=0}^{n-1}\sum_{j=1}^{4} b_j k(t, t_l + c_j h, X_{l,j}), \qquad n = 1, ..., N-1,$$

where $B = \int_0^b k(t, s, x(s))\, ds$ is computed using Simpson's Rule. The approximations are displayed in Figure 3.5. Note that the approximations of the two methods are very similar.

Since the exact solution of this problem cannot be computed for $t \in [0, 5]$, we measure the accuracy of our two methods against the averaging and linear spline schemes for solving delay differential equations. More details of the average scheme can be found in [4], see [5,10 and 14] for details of the spline schemes. The average and spline schemes are well known to be accurate. Thus, it is apparent from Figure 3.6 that our internal state and direct numerical methods are very precise for $t > 0$. We then compare the computing time between these four numerical methods on the interval $t \in [0, 5]$ with the results given in Table 3.2. It is obvious from Table 3.2 that the direct numerical method requires the most computing time while the internal state method requires the least amount of computing time among the four methods mentioned.

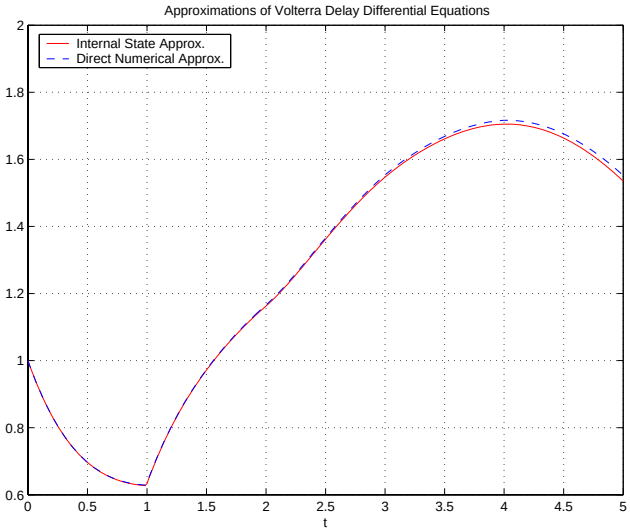

Figure 3.5: Volterra delay differential equation with cosine kernel (N = 64)

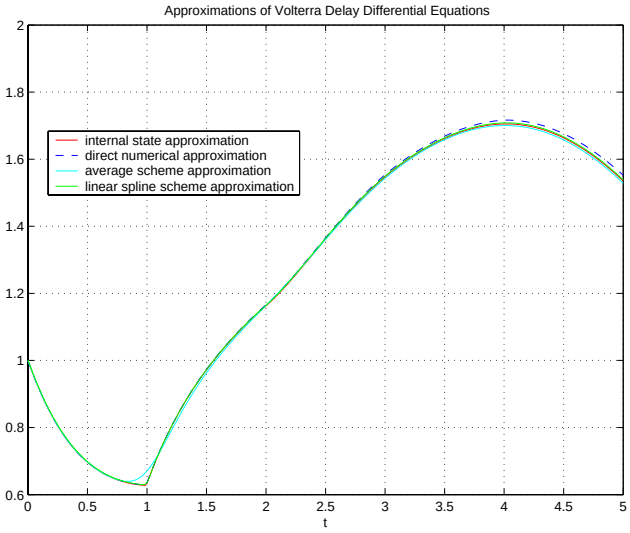

Figure 3.6: Approximations using the four methods for cosine kernel (N = 64)

N	Internal State Method	Direct Numerical Method	Average Scheme	Linear Spline Scheme
4	0.0200	0.0700	0.2000	0.2700
8	0.0300	0.1510	0.2500	0.4210
16	0.0500	0.4700	0.4010	0.6510
32	0.0900	1.5730	0.5410	1.1410
64	0.1710	5.9180	1.0110	2.2530

Table 3.2: Computing time of four numerical methods in seconds.

3.4 Volterra Integro-differential Equation with Bounded-Realizable Kernel

This example illustrates a Volterra integro-differential equation where the kernel is realizable by delay differential equations. Thus, we apply the internal state method and compare it with the direct numerical method. The numerical approximations from both the internal state method and the direct numerical method are also compared against the exact solution. We report the computing time for each method.

Consider a Volterra integro-differential equation

$$\begin{aligned} \dot{x}(t) &= -x(t) + \int_0^t K(t-s)x(s)\,ds \qquad t > 0, \\ x(0) &= 1, \\ \text{where } K(\alpha) &= \begin{cases} 0, & \alpha < 1, \\ \alpha - 1, & \alpha \geq 1. \end{cases} \end{aligned} \tag{3.10}$$

To apply the internal state method to this problem, we show that the kernel $K(\alpha)$ is realized by a bounded realization. Taking the Laplace transform of $K(\alpha)$, we find

$$\mathcal{L}(K(\alpha))(s) = \hat{K}(s) = \frac{e^{-s}}{s^2}, \tag{3.11}$$

and as mentioned in [11] $\hat{K}(s) = \frac{e^{-s}}{s^2}$ is realizable. For verification, we demontstrate that $\hat{K}(s)$ satisfies all the sufficient conditions to be realizable.

Lemma 3.1

$$\hat{K}(s) = \frac{e^{-s}}{s^2} \in H^2(\Pi_\rho^+).$$

Proof: We need to show:

$$\sup_{x>\rho} \int_{-\infty}^{\infty} \left| \frac{e^{-(x+iy)}}{(x+iy)^2} \right|^2 dy < \infty.$$

For $\rho > 0$ fixed, we have

$$\begin{aligned}
\sup_{x>\rho} \int_{-\infty}^{\infty} \left| \frac{e^{-(x+iy)}}{(x+iy)^2} \right|^2 dy &\leq \sup_{x>\rho} \int_{-\infty}^{\infty} \frac{|e^{-2x}|\,|e^{-2iy}|}{|x^2+2ixy-y^2|^2}\, dy \\
&= \sup_{x>\rho} |e^{-2x}| \int_{-\infty}^{\infty} \frac{|e^{-2iy}|}{x^4+2x^2y^2+y^4}\, dy \\
&\leq \sup_{x>\rho} |e^{-2x}| \int_{-\infty}^{\infty} \frac{1}{(x^2+y^2)^2}\, dy \qquad \text{since } |e^{-2iy}| = 1 \\
&= \sup_{x>\rho} |e^{-2x}| \left[\int_{-1}^{1} \frac{1}{(x^2+y^2)^2}\, dy + \right. \\
&\qquad \left. \int_{-\infty}^{-1} \frac{1}{(x^2+y^2)^2}\, dy + \int_{1}^{\infty} \frac{1}{(x^2+y^2)^2}\, dy \right]
\end{aligned}$$

$$\begin{aligned}
&\leq \sup_{x>\rho} |e^{-2x}| \left[\int_{-1}^{1} \frac{1}{x^4}\, dy + \int_{-\infty}^{-1} \frac{1}{y^4}\, dy + \int_{1}^{\infty} \frac{1}{y^4}\, dy \right] \\
&\qquad \text{since the function is dominated by } \frac{1}{x^4} \text{ for } y \in [-1,1] \\
&\qquad \text{and } \frac{1}{y^4} \text{ otherwise} \\
&= \sup_{x>\rho} |e^{-2x}| \left[\frac{2}{x^4} - \frac{1}{3y^3}\Big|_{-\infty}^{-1} - \frac{1}{3y^3}\Big|_{1}^{\infty} \right] \\
&= \sup_{x>\rho} |e^{-2x}| \left[\frac{2}{x^4} + \frac{2}{3} \right] \\
&< |e^{-2\rho}| \left[\frac{2}{\rho^4} + \frac{2}{3} \right].
\end{aligned}$$

Furthermore, let $s \in \mathbb{C}$. We know e^{-s} and s^2 are differentiable for Re $s > 0$. Thus, for Re $s > 0$, $\hat{K}(s)$ is analytic and

$$\hat{K}'(s) = \frac{e^{-(s)}}{(s)^2} = \frac{-s^2e^{-s} - 2e^{-s}}{s^3}.$$

We conclude that $\hat{K}(s) = \frac{e^{-s}}{s^2} \in H^2(\Pi_\rho^+)$.

□

Lemma 3.2 *For $\hat{K}(s)$ defined in (3.11) and $K(t)$ defined in (3.10),*

$$s\hat{K}(s) - K(0) \in H^2(\Pi_\rho^+).$$

Proof: We need to establish

$$\sup_{x>\rho} \int_{-\infty}^{\infty} \left| \frac{e^{-(x+iy)}}{(x+iy)} \right|^2 dy < \infty$$

since $K(0) = 0$ and

$$s\hat{K}(s) = s\frac{e^{-s}}{s^2} = \frac{e^{-s}}{s}.$$

Fix $\rho > 0$, we have the following estimates

$$\begin{aligned}
\sup_{x>\rho} \int_{-\infty}^{\infty} \left| \frac{e^{-(x+iy)}}{(x+iy)} \right|^2 dy &\leq \sup_{x>\rho} \int_{-\infty}^{\infty} \frac{|e^{-2x}|\,|e^{-2iy}|}{x^2+y^2}\, dy \\
&= \sup_{x>\rho} |e^{-2x}| \int_{-\infty}^{\infty} \frac{|e^{-2iy}|}{x^2+y^2}\, dy \\
&\leq \sup_{x>\rho} |e^{-2x}| \int_{-\infty}^{\infty} \frac{1}{x^2+y^2}\, dy \qquad \text{where we have used } |e^{-2iy}| = 1 \\
&= \sup_{x>\rho} |e^{-2x}| \left[\int_{-1}^{1} \frac{1}{x^2+y^2}\, dy + \right. \\
&\qquad \left. \int_{-\infty}^{-1} \frac{1}{x^2+y^2}\, dy + \int_{1}^{\infty} \frac{1}{x^2+y^2}\, dy \right]
\end{aligned}$$

$$
\begin{aligned}
&\leq \sup_{x>\rho} |e^{-2x}| \left[\int_{-1}^{1} \frac{1}{x^2}\, dy + \int_{-\infty}^{-1} \frac{1}{y^2}\, dy + \int_{1}^{\infty} \frac{1}{y^2}\, dy \right], \\
&\quad \text{since the function is dominated by } \frac{1}{x^2} \text{ for } y \in [-1,1] \\
&\quad \text{and } \frac{1}{y^2} \text{ otherwise} \\
&= \sup_{x>\rho} |e^{-2x}| \left[\frac{2}{x^2} - \frac{1}{y}\Big|_{-\infty}^{-1} - \frac{1}{y}\Big|_{1}^{\infty} \right] \\
&= \sup_{x>\rho} |e^{-2x}| \left[\frac{2}{x^2} + 2 \right] \\
&< |e^{-2\rho}| \left[\frac{2}{\rho^2} + 2 \right].
\end{aligned}
$$

Similarly, let $h(s) = s$ on $\mathbb{C}$. Obviously h is differentiable for Re $s > 0$ and we know e^{-s} is also differentiable for Re $s > 0$. It follows that $s\hat{K}(s)$ is analytic for Re $s > 0$ and

$$[s\hat{K}(s)]' = \frac{-e^{-s}}{s^2} - \frac{e^{-s}}{s}.$$

□

Since the conditions in Lemma 3.1 and 3.2 hold, $K(\alpha)$ defined in (3.10) is realizable by Theorem 1.3.

Following the procedures in [15], we construct a delay system below as a realization of the kernel given in (3.10) above

$$
\begin{aligned}
\dot{z_1}(t) &= z_2(t-1) \\
\dot{z_2}(t) &= x(t) \\
z_1(0) &= 0, \qquad\qquad z_2(0) = 0,
\end{aligned}
\tag{3.12}
$$

and the history function $z_2(\gamma) = 0$ for $\gamma \in [-1, 0)$ since we consider only zero initial states.

It follows from the internal state method that the integro-differential equation (3.10) can be written as a delay differential equation (DDE) system

$$
\begin{aligned}
\dot{x}(t) &= -x(t) + z_1(t) \\
\dot{z_1}(t) &= z_2(t-1) \\
\dot{z_2}(t) &= x(t)
\end{aligned}
\tag{3.13}
$$

with initial conditions

$$x(0) = 1, \qquad z_1(0) = 0, \qquad z_2(0) = 0,$$

and initial function

$$z_2(\gamma) = 0 \qquad \gamma \in [-1, 0).$$

To verify the above DDE system (3.13) is equivalent to the integro-differential equation (3.10), we transform the system (3.12). That is,

$$\mathcal{L}\begin{pmatrix} \dot{z_1}(t) \\ \dot{z_2}(t) \end{pmatrix} = \mathcal{L}\begin{pmatrix} z_2(t-1) \\ x(t) \end{pmatrix} \text{ implies } \begin{array}{rcl} sZ_1(s) &=& e^{-s}Z_2(s) \\ sZ_2(s) &=& X(s). \end{array}$$

Here $Z_1(s)$, $Z_2(s)$, and $X(s)$ represent to be the Laplace transforms of $z_1(t)$, $z_2(t)$, and $x(t)$ respectively. Solving for Z_1, we get

$$Z_1(s) = \frac{e^{-s}}{s^2}X(s),$$

and by the convolution theorem,

$$z_1(t) = \int_0^t \mathcal{L}^{-1}\left(\frac{e^{-(t-\tau)}}{(t-\tau)^2}\right)x(\tau)d\tau$$

and

$$z_1(t) = \int_0^t K(t-\tau)x(\tau)d\tau, \tag{3.14}$$

where $K(\alpha)$ is defined in (3.10).

Another linear system that represents the Volterra integro-differential equation (3.10) above is

$$\begin{array}{rcl} \dot{x}(t) &=& -x(t) + z_2(t) \\ \dot{z_1}(t) &=& x(t) \\ \dot{z_2}(t) &=& z_1(t-1) \end{array} \tag{3.15}$$

with initial conditions

$$x(0) = 1, \qquad z_1(0) = 0, \qquad z_2(0) = 0$$

and initial function

$$z_1(\gamma) \;=\; 0, \qquad\qquad \gamma \in [-1, 0).$$

It is fairly straightforward to verify this system (3.15) generates the integro-differential equation (3.10). Using the same notation and following the same procedures as given above, we has

$$\begin{bmatrix} sZ_1(s) \\ sZ_2(s) \end{bmatrix} = \begin{bmatrix} X(s) \\ e^{-s}Z_1(s) \end{bmatrix}.$$

Solving for Z_2, we get

$$Z_2(s) = \frac{e^{-s}}{s^2}X(s)$$

and by the convolution theorem,

$$z_2(t) = \int_0^t \mathcal{L}^{-1}\left(\frac{e^{-(t-\tau)}}{(t-\tau)^2}\right)x(\tau)d\tau,$$

which implies

$$z_2(t) = \int_0^t K(t-\tau)x(\tau)d\tau \tag{3.16}$$

where $K(\alpha)$ is defined in (3.10). Again, since the initial states is 0, it is obvious that we can choose $z_1(\gamma) = 0$ for $\gamma \in [-1, 0)$. Since we have two realizations for a transfer function in this problem we note that realizations are not unique. Although there are multiple state representations for each transfer function, there exists only one minimal state representation upto change of bases in the state space. More discussion on minimal realizations of delay systems can be found in [15].

Figure 3.7 provides the numerical solutions of the two systems above using the linear spline scheme with $N = 64$. System 1 is linear system (3.13) and system 2 is linear system (3.15). Figure 3.8 displays the numerical solutions of these two systems using the average scheme while the results in Figure 3.9 are from a fourth order Runge-Kutta method. It is apparent that the approximate solutions from system (3.13) and (3.15) resulting from all three methods are similar.

Table 3.3 displays the computing time of three numerical schemes solving

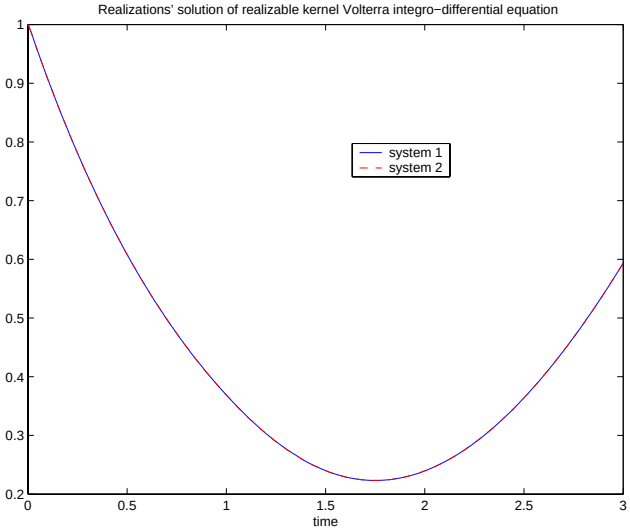

Figure 3.7: Linear spline solutions of the two linear systems (3.13) and (3.15) (N=64).

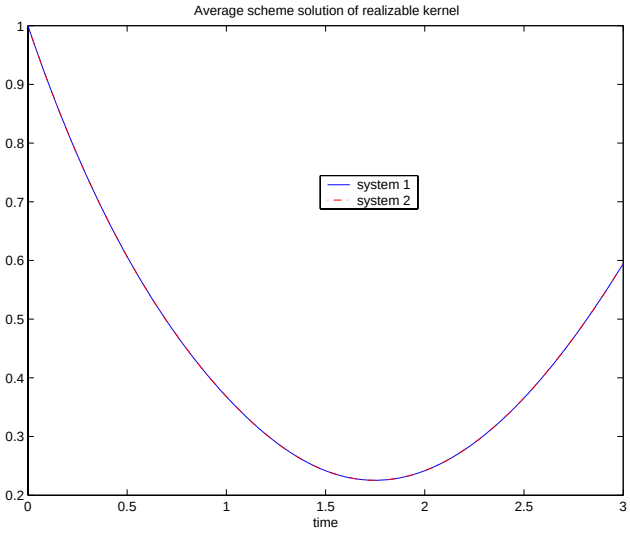

Figure 3.8: Average scheme solutions of the two linear systems (3.13) and (3.15) (N=64).

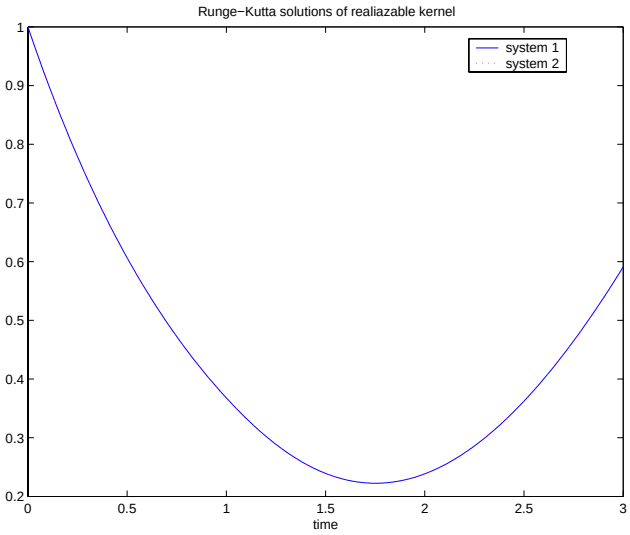

Figure 3.9: Runge-Kutta solutions of the two linear systems (3.13) and (3.15).

Numerical Methods	System 1 (3.13)	System 2 (3.15)
Runge-Kutta Method	0.1910	0.2100
Average Scheme	0.8610	0.8510
Linear Spline Scheme	2.3030	2.4130

Table 3.3: Computing time of three numerical schemes in seconds.

the two linear systems generated from the internal state method. The computing time of each numerical method does not vary much between the two systems. Runge-Kutta method is the most efficient of the three methods and the linear spline takes up the most computing time.

Integro-differential equation (3.10) can be solved by a change of variable and the method of steps. Let $w = t - s$, then equation (3.10) becomes

$$\begin{aligned} \dot{x}(t) &= -x(t) + \int_0^t K(w)x(t-w)dw, \qquad t > 0, \qquad (3.17) \\ x(0) &= 1. \end{aligned}$$

On the interval $[0, 1)$, equation (3.17) is simply

$$\dot{x}(t) = -x(t) \qquad (3.18)$$

since $K(s) = 0$ for $s \in [0, 1)$. With the initial condition, $x(0) = 1$, it follows that $x(t) = e^{-t}$ is the solution on $[0, 1)$. For $t \geq 1$, we split the integral in equation (3.17) into two integrals such as

$$\dot{x}(t) = -x(t) + \int_0^1 K(s)x(t-s)\,ds + \int_1^t K(s)x(t-s)\,ds. \qquad (3.19)$$

Substitute for $K(s)$ and with a change of variables, we are left with

$$\dot{x}(t) = -x(t) + \int_0^{t-1} (t-s-1)x(s)\,ds \qquad (3.20)$$

since $K(s) = 0$ for $s \in [0, 1)$ implies $\int_0^1 K(s)x(t-s)\,ds$ goes to 0.

Note that we can consider equation (3.19) as an equivalence of the original given integro-differential equation (3.10) for $t > 0$ if we assume $x(s) = 0$ for $s \in [-1, 0)$. On the interval where $t \in [1, 2)$, $x(s)$ for $s \in [0, t-1)$ is known as e^{-s}. So the integro-differential equation (3.10) given above now becomes

$$\begin{aligned} \dot{x}(t) &= -x(t) + \int_0^{t-1} (t-s-1)e^{-s}\,ds \qquad (3.21) \\ x(1) &= e^{-1}. \end{aligned}$$

Integrate $\int_0^{t-1}(t-s-1)e^{-s}\,ds$, and we simply have a non-homogenous ODE

$$\begin{aligned} \dot{x}(t) &= -x(t) + t + e^{(1-t)} - 2 \qquad (3.22) \\ x(1) &= e^{-1}. \end{aligned}$$

It follows that the solution of the ODE (3.22) above is

$$x(t) = t + te^{(1-t)} + (1+e)e^{-t} - 3. \tag{3.23}$$

Similarly, the ideas above can be used to solve for $x(t)$ for $t \in [n, n+1)$, where $n = 2, 3, ..., N$. So if we are looking at solving for $x(t)$ on the interval $[2, 3)$, we would have the integro-differential equation

$$\dot{x}(t) = -x(t) + \int_0^1 (t-s-1)e^{-s}\,ds + \int_1^{t-1} (t-s-1)(s+se^{(1-s)}+(1+e)e^{-s}-3)\,ds \tag{3.24}$$

with the initial condition

$$x(2) = e^{-2} + 3e^{-1} - 1.$$

Integrate all the integrals and then solve for the ODE above, and the solution on $[2, 3)$ yields

$$x(t) = (4e^2 + e + 1)e^{-t} + te^{(1-t)} + (\frac{t^2}{2} + 2t)e^{(2-t)} + \frac{1}{6}t^3 - \frac{5}{2}t^2 + 15t - (15 + \frac{104}{6}).$$

As for the direct numerical approximations, we consider equation (3.19) as an equivalent form of the given original integro-differential equation with the assumption that $x(s) = 0$ for $s \in [-1, 0)$, and the initial condition $x(0) = 1$. Define $g(t, x)$ to be $-x(t) + \int_0^t -1(t-s-1)x(s)\,ds$; we then approximate the solution $x(t)$ for $t \in [0, T]$ using explicit fourth order Runge-Kutta formulas

$$\begin{aligned} x_{n+1} &= x_n + \frac{h}{6}(K_1 + 2K_2 + 2K_3 + K_4) \\ K_1 &= g(t_n, x_n) \\ K_2 &= g(t_n + \frac{h}{2}, x_n + \frac{h}{2}K_1) \\ K_3 &= g(t_n + \frac{h}{2}, x_n + \frac{h}{2}K_2) \\ K_4 &= g(t_n + h, x_n + hK_3), \end{aligned}$$

where $x_n = x(t_n)$. We use Simpson's Rule to numerically calculate the integral. Note that Brunner and van der Howen's Runge-Kutta formulas cannot be used to directly approximate the solution for this problem because

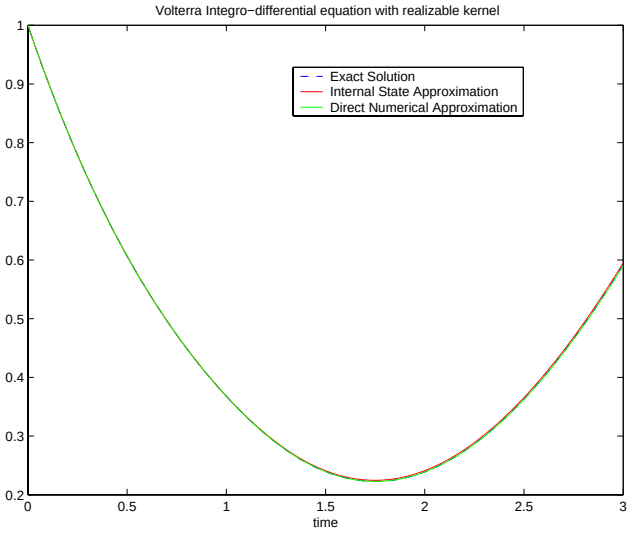

Figure 3.10: Exact solution and approximated solutions from internal state and direct numerical method (h=0.01)

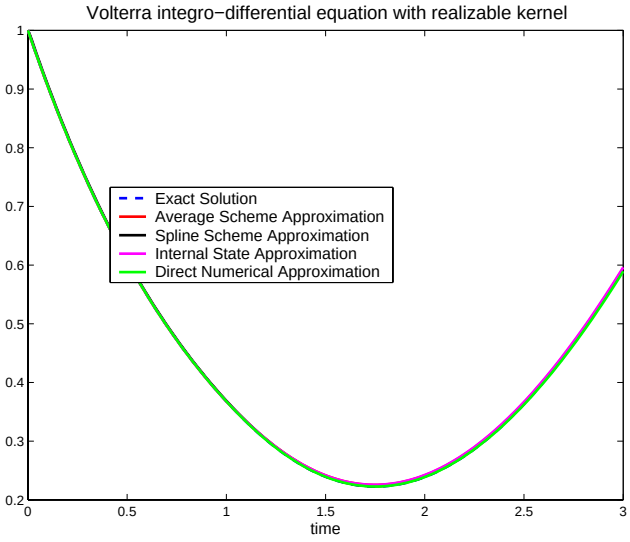

Figure 3.11: Exact solution and approximated solutions from four numerical schemes (N=64).

Numerical Methods	Computing Time
Internal State Method	0.1500
Direct Numerical Method	0.2500
Average Scheme	0.8520
Linear Spline Scheme	2.3430

Table 3.4: Computing time of four numerical methods in seconds with N=64.

$x(s)$ inside the integral is known in this example. Brunner and van der Howen's formulas consider the case where $x(s)$ in the integral is unknown.

Using the exact solution that was computed on each interval above, we can verify the performances of these two numerical schemes. Figure 3.10 is the plot of the exact solution versus the approximated solution from the internal state method and the direct numerical method on the interval from $[0, 3]$. Also, from Figure 3.10, it is obvious that these two numerical methods are highly accurate with the step size of $h = 0.01$. The averaging scheme and the linear spline scheme are also used to approximate the delay system (3.13). With the internal state method, explicit fourth order Runge-Kutta formulas are used with the method of steps to solve for the DDE system (3.13) since DDE systems (3.13) and (3.15) generate the same solution. Figure 3.11 plots the exact solution with the approximations from the averaging scheme, the linear spline schemes, and our two numerical methods for the step size of $h = 1/64$. From the figure, these four numerical methods are very precise since all the graphs lie on one another. We then observe the computing time for each method with $N = 64$ and, from Table 3.4, the internal state method is still faster compared to the other three methods. The direct numerical method is faster than the averaging and the linear spline schemes but it is still slower than the internal state method.

3.5 Volterra Integro-differential Equation Realizable Kernel

This example illustrates the case where the kernel of a Volterra integro-differential equation is not bounded-realizable [see 11] but realizable.

Consider

$$\begin{aligned} \dot{x}(t) &= -x(t) + \int_0^t K(t-s)x(s)\,ds \qquad t > 0, \\ x(0) &= 1, \\ \text{where } K(\alpha) &= \begin{cases} 0, & \alpha < 1, \\ 1, & \alpha \geq 1. \end{cases} \end{aligned} \tag{3.25}$$

Before we discuss the realizability of the kernel above, we now present the procedures for obtaining the exact solution of the Volterra system (3.25) since they are similar to the procedure used in the previous example. That is, the exact solution is solved by the method of steps and a couple changes of variable. After a change of variable, system (3.25) becomes

$$\begin{aligned} \dot{x}(t) &= -x(t) + \int_0^t K(s)x(t-s)\,ds \qquad t > 0, \\ x(0) &= 1. \end{aligned} \tag{3.26}$$

Then on the interval $[0, 1)$, we have

$$\begin{aligned} \dot{x}(t) &= -x(t) \\ x(0) &= 1, \end{aligned}$$

which yields $x(t) = e^{-t}$ as the solution and $x(1) = e^{-1}$.

For $t \in [1, 2)$, we split the integral limits in (3.26) from 0 to 1 and from 1 to t, substitute for $K(\alpha)$, and do another change of variable; we are left with an ODE system

$$\begin{aligned} \dot{x}(t) &= -x(t) + \int_0^{t-1} e^{-s}\,ds \\ x(1) &= e^{-1}. \end{aligned} \tag{3.27}$$

It follows that the solution for the ODE system (3.27) above is

$$x(t) = -te^{(1-t)} + e^{-t} + 1,$$

and

$$x(2) = 2e^{-1} + e^{-2} + 1.$$

Following the steps above, the solution $x(t)$ for $t \in [2, 3)$ is

$$x(t) = -3 - te^{(1-t)} + t - 1 + \frac{t^2}{2}e^{(2-t)} + (1 + e^2)e^{-t}.$$

The solution $x(t)$ can be solved for $t \in [n, n + 1)$, where $n = 2, 3, ..., N$ with the presented procedures.

As for realizability, it is obvious that $K(\alpha)$ is non-realizable if we retrict B and C to be bounded, since it does not have continuity, which is a necessary condition for $K(\alpha)$ to be realizable. However, if we allow either B or C to be unbounded then $K(\alpha)$ can be realizable.

Theorem 3.1

$$K(\alpha) = \begin{cases} 0, & \alpha < 1 \\ 1, & \alpha \geq 1 \end{cases}$$

is realizable.

Proof: Consider the Laplace transform of K above, that is

$$\hat{K}(s) = \frac{e^{-s}}{s}.$$

For $s > 0$, let $\mathbb{R}$ be the input space and $\mathbb{R}$ be the output space, then for $u_1, u_2 \in \mathbb{R}$ we want to show: $\hat{K}(s)$ is in $L(\mathbb{R}, \mathbb{R})$.

$$\begin{aligned} \hat{K}(s)(u_1 + u_2) &= \frac{e^{-s}}{s}(u_1 + u_2) \\ &= \frac{e^{-s}}{s}u_1 + \frac{e^{-s}}{s}u_2 \\ &= \hat{K}(s)u_1 + \hat{K}(s)u_2. \end{aligned}$$

Also, for $u \in \mathbb{R}$, and $\alpha \in \mathbb{R}$

$$\begin{aligned} \hat{K}(s)\alpha u &= \frac{e^{-s}}{s}\alpha u \\ &= \alpha\frac{e^{-s}}{s}u \\ &= \alpha\hat{K}(s)u. \end{aligned}$$

So $\hat{K}(s)$ is in $L(\mathbb{R},\mathbb{R})$. As for $\hat{K}(s)$ being uniformly bounded on $L(\mathbb{R},\mathbb{R})$ we need to fix $s=\beta>0$ and look at

$$\begin{aligned}
\|\hat{K}(s)\| &= \max_{u\in\mathbb{R}\setminus\{0\}} \frac{\|\hat{K}(s)u\|_{\mathbb{R}}}{\|u\|_{\mathbb{R}}} \\
&= \max_{u\in\mathbb{R}\setminus\{0\}} \frac{\|\frac{e^{-s}}{s}u\|_{\mathbb{R}}}{\|u\|_{\mathbb{R}}} \\
&\leq \max_{u\in\mathbb{R}\setminus\{0\}} \frac{\|\frac{e^{-s}}{s}\|_{\mathbb{R}}\|u\|_{\mathbb{R}}}{\|u\|_{\mathbb{R}}} \\
&= \left\|\frac{e^{-s}}{s}\right\|_{\mathbb{R}} \\
&< \left|\frac{e^{-\beta}}{\beta}\right|.
\end{aligned}$$

From Section 3.3, it is obvious that $\hat{K}(s)$ is analytic on $\{s\in\mathbb{C}|\ \text{Re}\ s>0\}$ and

$$\hat{K}'(s)=-\frac{e^{-s}}{s^2}-\frac{e^{-s}}{s}.$$

In order to show the limit of $\hat{K}$ exists, we need to show

$$\lim_{x\to\infty}\max\ y\|\hat{K}(x+iy)\|=\hat{K}(\infty)<\infty.$$

Consider

$$\begin{aligned}
\lim_{x\to\infty}\max\ y\|\hat{K}(x+iy)\| &= \lim_{x\to\infty}\max\ y\left|\frac{e^{-(x+iy)}}{x+iy}\right| \\
&= \lim_{x\to\infty}\max\ y\frac{|e^{-x}e^{-iy}|}{|x+iy|} \\
&= \lim_{x\to\infty}\max\ y\frac{|e^{-x}e^{-iy}|}{\sqrt{x^2+y^2}} \\
&\leq \lim_{x\to\infty}\ y\frac{|e^{-x}|}{x}
\end{aligned} \tag{3.28}$$

$$\begin{aligned} &= y \lim_{x\to\infty} \frac{|e^{-x}|}{x} \\ &= 0. \end{aligned}$$

It follows from Theorem 1.4 in [21] that $K(\alpha)$ is realizable.

□

One realization that $K(\alpha)$ generates is

$$\begin{aligned} \dot{z}(t) &= x(t-1) \\ z(0) &= 0. \end{aligned} \tag{3.29}$$

Note that we do not have the initial history stated here since this realization requires the history of, x, given in (3.25) which we only have informations for $t \geq 0$. It is possible to put the history on x but it is not obvious what $x(\gamma)$ should be for $\gamma \in [-1, 0)$.

In verification that (3.29) is the state representation of $K(\alpha)$, consider the Laplace transform of

$$\mathcal{L}(\dot{z}(t)) = \mathcal{L}(x(t-1)). \tag{3.30}$$

We denote $Z(s)$ and $X(s)$ to be the Laplace transform of $z(t)$ and $x(t)$ respectively. It follows that

$$Z(s) = \frac{e^{-s}}{s} X(s),$$

and using the convolution theorem, the solution is given by

$$z(t) = \int_0^t \mathcal{L}^{-1}\left(\frac{e^{-(t-\tau)}}{(t-\tau)}\right) x(\tau)\, d\tau,$$

which is the integral part of Volterra system (3.25). Here the input operator B is not bounded but has a time delay and the ouput operator C is bounded. It follows that the linear system below represents the Volterra integro-equation (3.25)

$$\begin{aligned} \dot{x}(t) &= -x(t) + z(t) \\ \dot{z}(t) &= x(t-1) \\ x(0) &= 1 \\ z(0) &= 0, \end{aligned} \tag{3.31}$$

The solution $x(t)$ of system (3.31) is dependent on what we pick for the initial function since we have a DDE system whose solution is uniquely determined by the history function. Another realization

$$\begin{aligned} \dot{z}(t) &= x(t) \\ y(t) &= z(t-1) \\ z(0) &= 0. \end{aligned} \tag{3.32}$$

also produces the integral part of system (3.25). With this realization, it is natural to chose $z(\gamma) = 0$ for $\gamma \in [-1, 0)$ since, similar to the previous example, the internal variable $z(t)$ can be constructed to our convenience. Take the Laplace transform of system (3.32),

$$\mathcal{L}\begin{pmatrix} \dot{z}(t) \\ y(t) \end{pmatrix} = \mathcal{L}\begin{pmatrix} x(t) \\ z(t-1) \end{pmatrix},$$

then we have

$$Y(s) = \frac{e^{-s}}{s} X(s).$$

Applying the convolution theorem, we get

$$y(t) = \int_0^t \mathcal{L}^{-1}\left(\frac{e^{-(t-\tau)}}{(t-\tau)}\right) x(\tau)\, d\tau,$$

and $y(t)$ is the integral of system (3.25) above.

Thus, the linear system

$$\begin{aligned} \dot{x}(t) &= -x(t) + z(t-1) \\ \dot{z}(t) &= x(t) \\ x(0) &= 1 \\ z(0) &= 0 \\ z(\gamma) &= 0 \qquad \gamma \in [-1, 0), \end{aligned} \tag{3.33}$$

also generates the Volterra integro-differential equation (3.25). Here, unlike system (3.29), the input operator B of system (3.32) is bounded but the output operator C involves a time delay. Again, having two realizations in this problem illustrates the non-uniqueness of realizations.

Figure 3.12, 3.13, and 3.14 provide the solutions of the two corresponding DDE systems (3.31) and (3.33) to the Volterra equation (3.25) using the linear spline scheme, the average scheme and fourth-order Runge-Kutta method

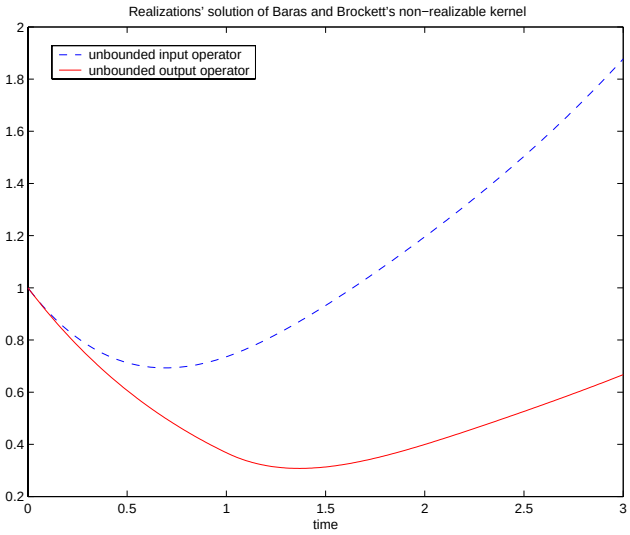

Figure 3.12: Solutions of two corresponding systems generating by linear spline scheme with history of x(s)=1 (N=64)

respectively. The initial function $x(\gamma)$ of system (3.31) is randomly selected to be 1 for $\gamma \in [-1, 0)$. N is chosen to be 64 for Figure 3.12 and 3.13 and $h = 1/64$ is the step size we use for Figure 3.14. Furthermore, for Figure 3.13 and 3.14, system 1 corresponds to system (3.31) and system 2 is the DDE system (3.33). We show the solutions of system (3.31) and (3.33) in Figure 3.12, 3.13, and 3.14 to verify the three methods mentioned above provide the same solutions. Notice from the three plots that these two systems, which generate the same Volterra system, give different solutions. Since the initial function $x(\gamma)$ of system (3.31) is not explicitly defined, we believe it can be chosen to produce the same solution as system (3.33). However, before we force the unbounded input system (3.31) to produce the same solution as system (3.33), we need to know which of the two solutions match with the exact solution determined from the integro-differential equation (3.25). The answer to that question is given in Figure 3.15, which implies the numerical solution from system (3.33) is very closed to the exact solution of Volterra equation (3.25). Also, the numerical scheme that is used in Figure 3.15 is the linear spline scheme with $N = 64$.

We now need to find the appropriate initial function $x(\gamma)$ for $\gamma \in [-1, 0)$ in system (3.31) to force its solution to match with the solution of system (3.33).

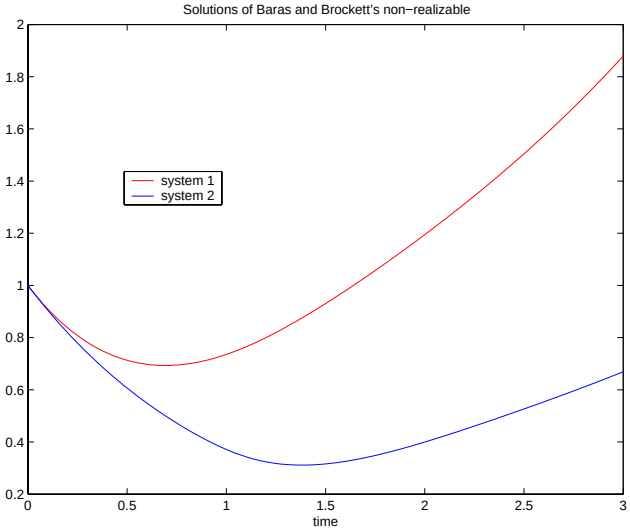

Figure 3.13: Solutions of two corresponding linear systems using average scheme with history of x(s)=1 (N=64)

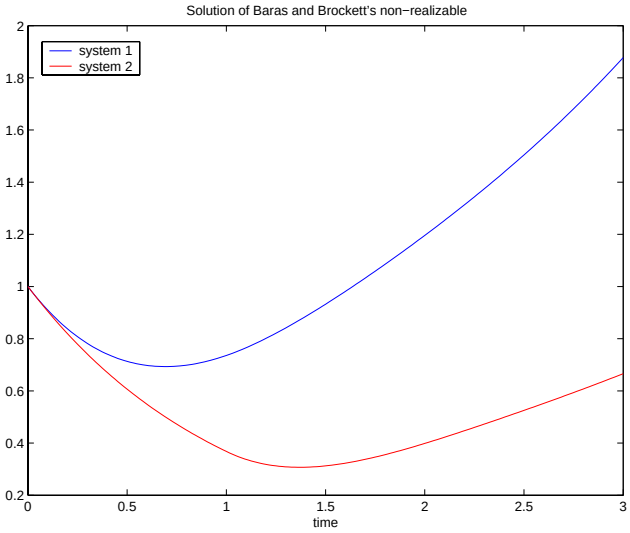

Figure 3.14: Solutions of two corresponding linear systems using Runge-Kutta method and history of x(s)=1 (N=64)

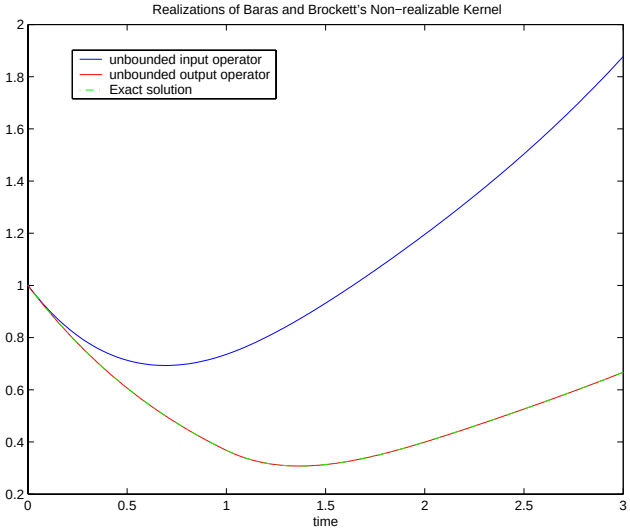

Figure 3.15: Solutions of two corresponding linear systems with history of x(s)=1 and the exact solution of Volterra system (3.25) (N=64)

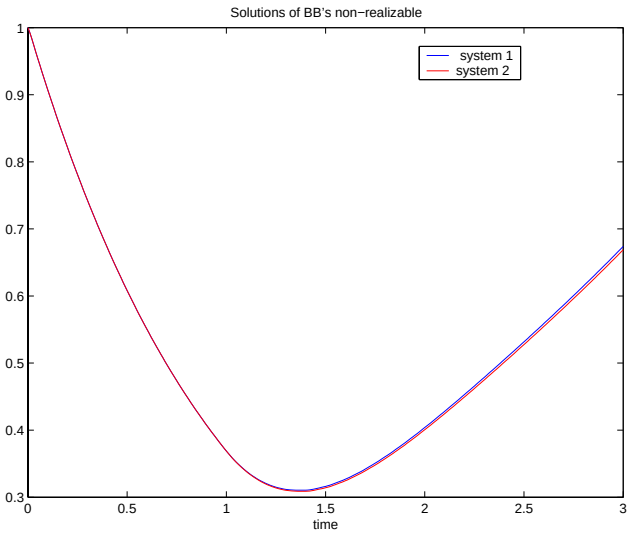

Figure 3.16: Solutions of two corresponding systems generating by linear spline scheme with history of x(s)=0 (N=64)

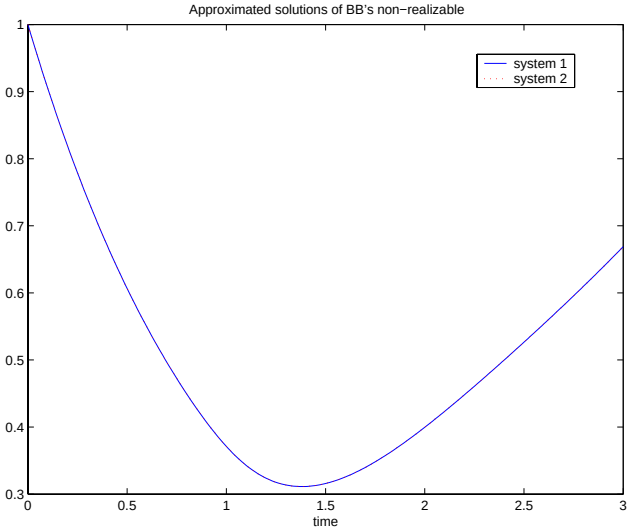

Figure 3.17: Solutions of two corresponding linear systems using average scheme with history of x(s)=0 (N=64)

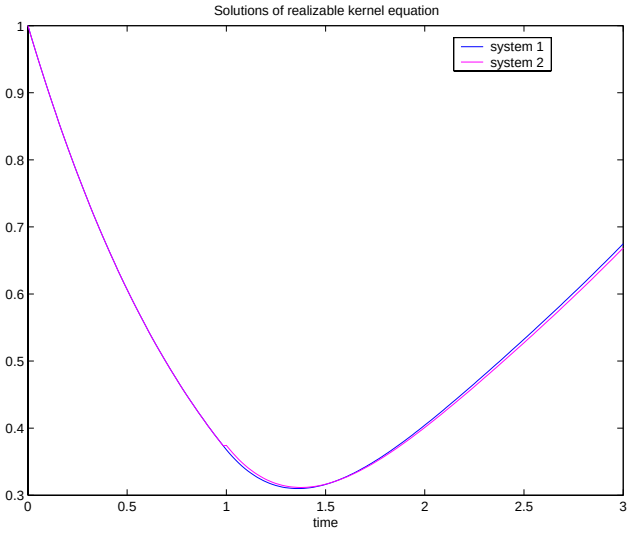

Figure 3.18: Solutions of two corresponding linear systems using Runge-Kutta method and history of x(s)=0 (N=64)

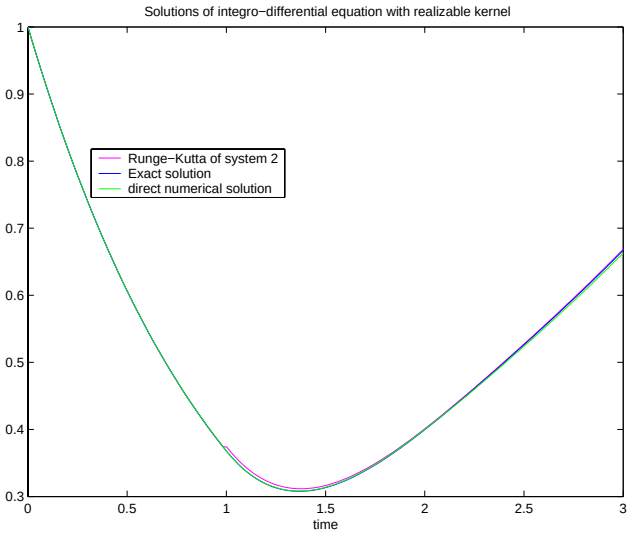

Figure 3.19: Solutions of Volterra integro-differential equation with realizable kernel (N=64)

By observation we select $x(\gamma) = 0$ for $\gamma \in [-1, 0)$, since with $z(0) = 0$, $z(t)$ yields to be 0 on $t \in [0, 1)$. It follows that the differential equation in system (3.31) is identical to the equation in system (3.33) for $t \in [0, 1)$. We numerically solve system (3.31) with a new history function and system (3.33) using the linear spline scheme, the average scheme and the Runge-Kutta method. Figure 3.16, 3.17, and 3.18 are the approximated solutions from the linear spline scheme, the average scheme and the Runge-Kutta method respectively. N again is chosen to be 64 for the linear spline and the average schemes and h is chosen to be $1/64$ for the Runge-Kutta method. Once again, system 1 in the plots is DDE system (3.31) and system 2 is DDE system (3.33). From the three figures, it is apparent that with $x(\gamma)$ chosen to be 0 for $\gamma \in [-1, 0)$, the two linear systems provide the same numerical approximations. Even though the approximations from three methods are highly accurate, it is obvious from Figure 3.17 that the average scheme provides the best estimation compared to the other two numerical methods. From the results in Figure 3.16, 3.17, and 3.18, we conclude that with realizations where initial conditions do not fall out naturally, we can choose suitable initial conditions to have the most precise approximations from the realizations. From this example, we learn that we should pick the linear system where all the initial

Numerical Methods	System 1 (3.31)	System 2 (3.33)
Runge-Kutta Method	0.1510	0.0910
Average Scheme	0.6210	0.6410
Linear Spline Scheme	1.4220	1.4120

Table 3.5: Computing time of three numerical schemes in seconds.

conditions comes out naturally from realization theory and the internal state method to approximate for the given Volterra system.

The computing times of Runge-Kutta, average, and linear spline schemes for the two systems (3.31) and (3.33), for $x(\gamma) = 1$ when $\gamma \in [-1, 0)$, are in Table 3.5. Again, the difference of computing time between the two system of each method is very small; the Runge-Kutta method is the most efficient between the three methods. We do not have a computing time table for these three methods with $x(\gamma) = 0$ when $\gamma \in [-1, 0)$ because there is no change in the algorithms, so the computing times should be the same as in Table 3.5. Figure 3.19 provides numerical solutions of the Runge-Kutta method of system (3.33), the direct numerical method, and the exact solution of the Volterra integro-differential equation (3.25). The step size that is used in Figure 3.19 is $h = 1/64$. From Figure 3.19, the internal state method and the direct numerical method generate very accurate approximations. The direct numerical method takes 0.2200 seconds to compute for $h = 1/64$. Comparing the computing time of the direct numerical method with the times of other methods in Tabe 3.5, we findthe internal state method is still a little faster than the direct numerical method in this problem.

3.6 Time-Dependent Kernel

All the problems above imply that the internal state method is more efficient than the direct numerical method. Furthermore, the kernels of all the prolems above are of convolution type and they all realize time invariant linear systems. Therefore, we generate an example of a Volterra delay differential equation with a non-convolution kernel that realizes a time variant linear system to study the efficiency of the two methods.

Consider a Volterra delay differential equation

$$\begin{aligned} \dot{x}(t) &= x(t) + x(t-1) + \int_0^t e^{s^2-t^2} x(s)\, ds \qquad t > 0, \\ x(\tau) &= \frac{4}{9} - \frac{2}{3}\tau - \frac{1}{9}e^{3(\tau+1)}, \qquad \tau \in [-1, 0), \\ x(0) &= 0. \end{aligned} \tag{3.34}$$

By the internal state method, the DDE system corresponding to (3.34) is

$$\begin{aligned} \dot{x}(t) &= x(t) + x(t-1) + z(t) \qquad (3.35) \\ \dot{z}(t) &= -2tz(t) + x(t) \\ x(0) &= 0 \\ z(0) &= 0 \qquad (3.36) \\ x(\tau) &= \frac{4}{9} - \frac{2}{3}\tau - \frac{1}{9}e^{3(\tau+1)}, \qquad \tau \in [-1, 0), \end{aligned}$$

since the integral in (3.34) is the solution of

$$\dot{z}(t) = -2tz(t) + x(t)$$

with the initial condition

$$z(0) = 0.$$

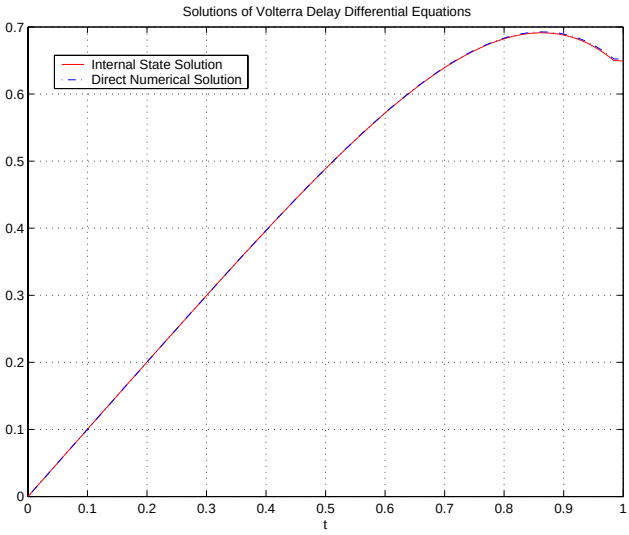

Figure 3.20: Time-variant problem (N=64)

Figure 3.20 plots the two numerical solutions of the delay differential equation (3.34). The direct numerical method takes 1.3420 seconds to compute while the internal state method only requires 0.1700 seconds. The computing times of these two methods for this problem indicate that even with a non-convolutional kernel that generates a time variant linear system, it requires less time to approximate the corresponding DDE system than approximating the Volterra delay differential equation directly.

Chapter 4

Approximate Realization

4.1 Hankel and Riesz-Spectral Operators

This section presents background and results on Hankel and Riesz-spectral operators that are necessary for the next two sections in Chapter 4. The first subsection below focuses on Hankel operators and the second subsection is concentrated on Riesz-spectral operators.

4.1.1 Hankel Operators

This subsection will cite all the necessary definitions and theorems from Glover et al. [see 20] as our tools to derive the results in the next section.

Consider a class of linear, infinite-dimensional systems defined by the following input-output map

$$y(t) = \int_0^t h(t-s)u(s)\,ds, \tag{4.1}$$

where the outputs $y \in L_2(0,\infty;\mathbb{C}^p)$, while the inputs $u \in L_2(0,\infty;\mathbb{C}^m)$ and the impulse response satisfies

$$h \in L_1 \cap L_2(0,\infty;\mathbb{C}^{p\times m}).$$

The corresponding Hankel operator $\Gamma : L_2(0,\infty;\mathbb{C}^m) \to L_2(0,\infty;\mathbb{C}^p)$ is defined by

$$(\Gamma u)(t) = \int_0^\infty h(t+s)u(s)ds. \tag{4.2}$$

Definition 4.1 *A Hilbert space realization of the Hankel operator* Γ *(as defined in (4.2)) is a triple* $(C, T(t), B)$*, where* $T(t)$ *is a* C_0 *semigroup in the Hilbert space* H *(with infinitesimal generator* A*),* $B : \mathbb{C}^m \to D(A^*)^*$*, and* $C : D(A) \to \mathbb{C}^p$*.*

□

Note that $D(A) \subset H \subset D(A^*)^*$, and $T(t)$ restricts to a C_0 semigroup on $D(A)$ and has a unique extension to a C_0 semigroup on $D(A^*)^*$. We employ A^* to be the adjoint of A.

It follows that the infinite-dimenional linear systems of the input-output map in (4.1) can be written as

$$\begin{aligned} \dot{z}(t) &= Az(t) + Bx(t) \\ z(0) &= 0 \\ y(t) &= Cz(t), \end{aligned} \tag{4.3}$$

where x and y are the input and output, respectively, defined above and $z \in X$, the state space, such that $X = L_2(0, \infty)$. The operators A, B, and C are also defined as in Definition 4.1 above.

Definition 4.2 *The infinite-dimensional linear system (4.1) is of nuclear type if it determines a bounded Hankel operator* Γ *whose singular values satisfy*

$$\sum_1^\infty \sigma_i < \infty.$$

□

Theorem 4.1 *Suppose that* $h \in L_1 \cap L_2$ *is of nuclear type and either*
(i) h *is purely real, or*
(ii) h *is complex,* $\dot{h}$ *exists (in the sense that* h *is the integral of its derivative) and* $\dot{h}$ *is the kernel of a bounded Hankel operator.*
Then

$$\begin{aligned} &(a) \qquad \|\Gamma - \Gamma_n\|_N \to 0; \\ &(b) \qquad \|h - h_n\|_1 \to 0; \\ &(c) \qquad \|h - h_n\|_2 \to 0. \end{aligned}$$

□

Here we denote $\|\Gamma\|_N$ to be $\sum_{i=1}^{\infty} \sigma_i$, the nuclear norm of Γ and $\|h\|_1$, $\|h\|_2$ to be the regular $L_1(0,\infty)$, $L_2(0,\infty)$ norms of h, respectively. The convergence of h in the $L_2(0,\infty)$ norm in Theorem 4.1 above is essential to derive the results in Section 4.2. Note that the results Glover et al. attained consider operators B and C in system (4.3) to be bounded.

4.1.2 Riesz-Spectral Operators

In this subsection, we consider results regarding Riesz-spectral operators. We employ the following definitions and results from the semigroup section in [17] for future use in Section 4.3. Detailed explanations and proofs of the following results can be found in [17].

Definition 4.3 *A sequence of vectors $\{\phi_n, n \geq 1\}$ in a Hilbert space X forms a Riesz basis for X if the following two conditions hold:*

(a) $\overline{span}_{n\geq 1}\{\phi_n\} = X$;

(b) There exists positive constants m and M such that for arbitrary $N \in \mathbb{N}$ and arbitrary scalars α_n, $n = 1, 2, ..., N$, we have

$$m \sum_{n=1}^{N} |\alpha_n|^2 \leq \| \sum_{n=1}^{N} \alpha_n \phi_n \|^2 \leq M \sum_{n=1}^{N} |\alpha_n|^2.$$

□

Definition 4.4 *Suppose that A is a linear, closed operator on a Hilbert space, X, with simple eigenvalues $\{\lambda_n, n \geq 1\}$ and suppose that the corresponding eigenvectors $\{\phi_n, n \geq 1\}$ form a Riesz basis in X. If the closure of $\{\lambda_n, n \geq 1\}$ is totally disconnected, then we call A a Riesz-spectral operator.*

□

Note that totally disconnected means that no points λ, $\mu \in \overline{\{\lambda_n, n \geq 1\}}$ can be joined by a segment lying entirely in $\overline{\{\lambda_n, n \geq 1\}}$. Also, we denote $\langle \phi_n, \psi_m \rangle = \delta_{mn}$ for $\{\phi_n\}$, $\{\psi_n\}$ being *biorthogonal*.

Theorem 4.2 *Suppose that A is a Riesz-spectral operator with simple eigenvalues $\{\lambda_n, n \geq 1\}$ and corresponding eigenvectors $\{\phi_n, n \geq 1\}$. Let $\{\psi_n, n \geq 1\}$ be the eigenvectors of A^* such that $\langle \phi_n, \psi_m \rangle = \delta_{mn}$. Then A satisfies:*

(a) $\rho(A) = \{\lambda \in \mathbb{C} \mid \inf_{n \geq 1} |\lambda - \lambda_n| > 0\}$, $\sigma(A) = \overline{\{\lambda_n, n \geq 1\}}$ and for $\lambda \in \rho(A)$, $(\lambda I - A)^{-1}$ is given by

$$(\lambda I - A)^{-1} = \sum_{n=1}^{\infty} \frac{1}{\lambda - \lambda_n} \langle \cdot, \psi_n \rangle \phi_n;$$

(b) A has the representation

$$Az = \sum_{n=1}^{\infty} \lambda_n \langle z, \psi_n \rangle \phi_n$$

for $z \in D(A)$, and

$$D(A) = \{z \in X \mid \sum_{n=1}^{\infty} |\lambda_n|^2 \, |\langle z, \psi_n \rangle|^2 < \infty\};$$

(c) A is the infinitesimal generator of a C_0-semigroup, $T(t)$, if and only if

$$\sup_{n \geq 1} Re(\lambda_n) < \infty$$

and $T(t)$ is given by

$$T(t) = \sum_{n=1}^{\infty} e^{\lambda_n t} \langle \cdot, \psi_n \rangle \phi_n;$$

(d) The growth bound of the semigroup is given by

$$\omega_0 = \inf_{t>0}\left(\frac{1}{t}\log\|T(t)\|\right) = \sup_{n\geq 1} Re\ (\lambda_n).$$

□

Definition 4.5 and Theorem 4.3 and 4.4 below are cited from the input-output maps section in [17] letting operator $D = 0$.

Definition 4.5 *Consider the state linear system (4.3), denoted $\sum(A, B, C)$, with zero initial state. If there exists a real α such that $\hat{y}(s) = G(s)\hat{u}(s)$ for $Re\ (s) > \alpha$, where $\hat{u}(s)$ and $\hat{y}(s)$ are the Laplace transform of input u and output y, respectively, and $G(s)$ is a $L(U, Y)$-valued function of a complex variable defined for $Re\ (s) > 0$, then we call*

(a) $G(s)$ the transfer function of $\sum(A, B, C)$.

(b) The impulse response h of $\sum(A, B, C)$ is the inverse Laplace transform of G.

□

Theorem 4.3 *The transfer function G and the impulse response h of the state linear system $\sum(A, B, C)$ exist and are given by*

$$G(s) = C(sI - A)^{-1}B \qquad s \text{ in } \rho_\infty(A), \tag{4.4}$$

where $\rho_\infty(A)$ is the component of the resolvent set of A that contains an interval $[r, \infty)$, and for $T(t)$ be the C_0 semigroup

$$h(t) = \begin{cases} CT(t)B, & t \geq 0, \\ 0, & t < 0. \end{cases}$$

□

Theorem 4.4 *Let A be a Riesz-spectral operator. Suppose that $B \in L(\mathbb{C}^m, Z)$, $C \in L(Z, \mathbb{C}^p)$. The transfer function and impulse response of $\sum(A, B, C)$ are given by*

$$G(s) = \sum_{n=1}^{\infty} \frac{1}{s - \lambda_n} C\phi_n \overline{(B^*\psi_n)}^T \qquad \text{for } s \in \rho(A),$$

$$h(t) = \begin{cases} \sum_{n=1}^{\infty} e^{\lambda_n t} C\phi_n \overline{(B^*\psi_n)}^T, & t \geq 0 \\ 0, & t < 0. \end{cases}$$

□

Note that the formulas for transfer function $G(s)$ of a Riesz-spectral operator A in Theorem 4.4 is constructed from (4.4) in Theorem 4.3 and Theorem 4.2(a).

4.2 Approximations of Volterra Integro-differential Equations

One problem in realization theory is constructing the state representations from a *weighting pattern* or a *transfer function*. With a given kernel that is realizable, it is sometimes difficult to construct a state representation for it; thus, it is challenging to approximate the solution for a given Volterra integro-differential equation by the internal state method. With the results from this section, we can overcome that obstacle by approximating the transfer function and building a corresponding linear system from that. It is shown that the solution from the constructed linear system converges to the actual solution of the Volterra integro-differential equation. In fact, there are cases where this approach is more efficient in computing time than some numerical schemes of the existing realization.

Consider an abstract Volterra integro-differential equation of the form

$$\begin{aligned} \dot{x}(t) &= f(t) + \int_0^t K(t-s)x(s)\,ds \qquad 0 < t \leq T \\ x(0) &= \eta \in \mathbb{R}^m, \end{aligned} \tag{4.5}$$

where $x \in L_2(0,T;\mathbb{R}^m)$, $f \in L_2(0,T;\mathbb{R}^m)$ and $K \in L_1 \cap L_2(0,T;\mathbb{R}^{p\times m})$.

Lemma 4.1 *Suppose K defined in system (4.5) is of nuclear type, then*

$$\|y - y_n\|_2 \to 0 \tag{4.6}$$

where

$$y(t) = \int_0^t K(t-s)x(s)\,ds$$

and

$$y_n(t) = \int_0^t K_n(t-s)x(s)\,ds$$

Proof: We define

$$y^1(t) = \int_0^t K(t-s)x(s)\,ds$$

and note that we can extend $y^1(t)$ over the domain $(0,\infty)$ as $y(t)$ in (4.1), by

$$y^1(t) = \int_0^t K(t-s)x(s)\,ds + \int_t^\infty K(t-s)x(s)\,ds$$

where

$$\int_t^\infty K(t-s)x(s)\,ds = 0.$$

Furthermore, for the input $x \in L_2(0,T;\mathbb{R}^m)$ and the impulse response $K \in L_1 \cap L_2(0,T;\mathbb{R}^{p\times m})$ to share the domains of the input u and the impulse response h in (4.1), we set $x = 0$ and $K = 0$ for $t > T$. It follows that $y^1 \in L_2(0,T;\mathbb{R}^p)$. Since K is assumed to be of nuclear type and purely real, it follows from Theorem 4.1 above that

$$\|K - K_n\|_2 \to 0.$$

That is, $C_nT_n(t)B_n \to CT(t)B$ in the $L_2(0,T)$ norm [see 20]. In other words, we have a linear system

$$\begin{aligned} \dot{z}(t) &= Az(t) + Bx(t) \\ z(0) &= 0 \\ y^1(t) &= Cz(t), \end{aligned} \tag{4.7}$$

where A is an infinitesimal generator of a C_0 semigroup $T(t)$, $B : \mathbb{R}^m \to D(A^*)^*$, $C : D(A) \to \mathbb{R}^p$, and $D(A) \subset X = L_2(0,T)$, being approximated by system

$$\begin{aligned} \dot{z}_n(t) &= A_nz_n(t) + B_nx(t) \\ z_n(0) &= 0 \\ y_n^1(t) &= C_nz_n(t). \end{aligned} \tag{4.8}$$

Here, $A_n \in D(A)$ generate a C_0 semigroup $T_n(t)$ and $A_n \to A$. $B_n \in \mathbb{R}^m$ and $C_n \in D(A)$ such that $B_n \to B$ and $C_n \to C$ respectively.

By variation of parameters, $y_n^1(t)$ in system (4.8) can be solved as

$$y_n^1(t) = \int_0^t C_n T_n(t-s) B_n x(s)\, ds.$$

Now consider

$$\begin{aligned}
\|y^1 - y_n^1\|_2 &= \left\| \int_0^t K(t-s)x(s)\, ds - \int_0^t K_n(t-s)x(s)\, ds \right\|_2 \\
&= \left\| \int_0^t [K(t-s)x(s) - K_n(t-s)x(s)]\, ds \right\|_2 \\
&= \left(\int_0^T \left(\int_0^t [K(t-s) - K_n(t-s)]x(s) ds \right)^2 dt \right)^{\frac{1}{2}} \\
&\leq \left(\int_0^T \left(\left[\int_0^t [K(t-s) - K_n(t-s)]^2\, ds \right]^{\frac{1}{2}} \left[\int_0^t x^2(s)\, ds \right]^{\frac{1}{2}} \right)^2 dt \right)^{\frac{1}{2}} \\
&= \left(\int_0^T \left[\int_0^t [K(t-s) - K_n(t-s)]^2\, ds \int_0^t x^2(s)\, ds \right] dt \right)^{\frac{1}{2}} \\
&\leq \left[\left(\int_0^T \left[\int_0^t [K(t-s) - K_n(t-s)]^2\, ds \right]^2 dt \right)^{\frac{1}{2}} \left(\int_0^T \left[\int_0^t x^2(s)\, ds \right]^2 dt \right)^{\frac{1}{2}} \right]^{\frac{1}{2}}
\end{aligned}$$

since $t \in [0, T]$, we can interchange the order of integration and get

$$\begin{aligned}
&= \left[\left(\int_0^t \left[\int_0^T [K(t-s) - K_n(t-s)]^2\, ds \right]^{\frac{1}{2}} dt \right)^2 \left(\int_0^t \left[\int_0^T x^2(s)\, ds \right]^{\frac{1}{2}} dt \right)^2 \right]^{\frac{1}{2}} \\
&= \int_0^t \|K(t-s) - K_n(t-s)\|_2 \, \|x(s)\|_2\, ds.
\end{aligned}$$

Note that $\|K(t-s) - K_n(t-s)\|_2 \to 0$, so we have

$$\int_0^t \|K(t-s) - K_n(t-s)\|_2 \, \|x(s)\|_2\, ds$$

goes to 0 for all $t \leq T$.

□

Theorem 4.5 *Suppose K defined in system (4.5) is of nuclear type, then*

$$\|x - x_n\|_2 \to 0 \tag{4.9}$$

where $x(t)$ is the solution of system (4.5) above.

Proof: Let system (4.5) be given as $\dot{x}(t) = f(t) + y(t)$ where

$$y(t) = \int_0^t K(t-s)x(s)\,ds$$

and everything else is the same as in system (4.5). From Lemma (4.1) above, we know

$$y_n(t) = \int_0^t K_n(t-s)x(s)\,ds \tag{4.10}$$

exits and $\|y - y_n\|_2 \to 0$. It follows that we can contruct an approximate equation

$$\begin{aligned} \dot{x}_n(t) &= f(t) + y_n(t) \\ x_n(t) &= \eta \in \mathbb{R}^m. \end{aligned} \tag{4.11}$$

Obviously, $x_n(t) \in L_2(0, T; \mathbb{R}^m)$ and by variation of parameter,

$$x_n(t) = x_n(0) + \int_0^t [f(s) + y_n(s)]\,ds$$

and

$$x(t) = x(0) + \int_0^t [f(s) + y(s)]\,ds.$$

Then

$$\begin{aligned} \|x - x_n\|_2 &= \left\| \left[x(0) + \int_0^t [f(s) + y(s)]\,ds \right] - \left[x_n(0) + \int_0^t [f(s) + y_n(s)]\,ds \right] \right\|_2 \\ &= \left\| \int_0^t \Big(\big[f(s) - f(s)\big] + \big[y(s) - y_n(s)\big] \Big) ds \right\|_2 \\ &= \left\| \int_0^t \big[y(s) - y_n(s)\big] ds \right\|_2 \end{aligned}$$

$$
\begin{aligned}
&= \left[\int_0^T \left(\int_0^t \big[y(s) - y_n(s)\big] ds\right)^2 dt\right]^{\frac{1}{2}} \\
&\leq \left[\int_0^T \left(\left[\int_0^t 1^2\, ds\right]^{\frac{1}{2}} \left[\int_0^t \big[y(s) - y_n(s)\big]^2 ds\right]^{\frac{1}{2}}\right)^2 dt\right]^{\frac{1}{2}} \\
&= \left[\int_0^T \left(\int_0^t 1^2\, ds \int_0^t \big[y(s) - y_n(s)\big]^2 ds\right) dt\right]^{\frac{1}{2}} \\
&\leq \left(\left[\int_0^T \left(\int_0^t 1^2\, ds\right)^2 dt\right]^{\frac{1}{2}} \left[\int_0^T \left(\int_0^t \big[y(s) - y_n(s)\big]^2 ds\right)^2 dt\right]^{\frac{1}{2}}\right)^{\frac{1}{2}}
\end{aligned}
$$

interchanging the order of integration, we have

$$
\begin{aligned}
&= \left(\left[\int_0^t \left(\int_0^T 1^2\, ds\right)^{\frac{1}{2}} dt\right]^2 \left[\int_0^t \left(\int_0^T \big[y(s) - y_n(s)\big]^2 ds\right)^{\frac{1}{2}} dt\right]^2\right)^{\frac{1}{2}} \\
&\leq T^3 \int_0^t \|y(s) - y_n(s)\|_2 \, ds
\end{aligned}
$$

and $\|y(s) - y_n(s)\|_2 \to 0$ for $t \leq T$ implies $\|x - x_n\|_2 \to 0$ on $t \in [0, T]$.

□

Corollary 4.1 *Suppose an abstract Volterra integro-differential system is given in the form*

$$
\begin{aligned}
\dot{x}(t) &= f(x(t), t) + \int_0^t K(t-s)x(s)\, ds \qquad 0 < t \leq T \\
x(0) &= \eta \in \mathbb{R}^m,
\end{aligned} \tag{4.12}
$$

where $x \in L_2(0, T; \mathbb{R}^m)$, $f \in L_2(0, T; \mathbb{R}^m)$ *and* $K \in L_1 \cap L_2(0, T; \mathbb{R}^{p \times m})$.

If K *is of nuclear type and* f *is of Lipschitz condition (i.e.,* $\|f(x_1(s), s) - f(x_2(s), s)\|_2 \leq M \|x_1 - x_2\|_2$, *for* $M > 0$*), then*

$$\|x - x_n\|_2 \to 0.$$

Proof:

$$\begin{aligned}
\|x - x_n\|_2 &= \left\| \left[x(0) + \int_0^t [f(x(s), s) + y(s)]\, ds \right] - \left[x_n(0) + \int_0^t [f(x_n(s), s) + y_n(s)]\, ds \right] \right\|_2 \\
&= \left\| \int_0^t \Big(\big[f(x(s), s) - f(x_n(s), s) \big] + \big[y(s) - y_n(s) \big] \Big) ds \right\|_2 \\
&\leq \left\| \int_0^t \big[f(x(s), s) - f(x_n(s), s) \big] ds \right\|_2 + \left\| \int_0^t \big[y(s) - y_n(s) \big] ds \right\|_2
\end{aligned}$$

$f(x(s), s)$ is integrable over $[0, T]$ and using the same arguments presented above, we get

$$\begin{aligned}
&\leq \int_0^t \big\| f(x(s), s) - f(x_n(s), s) \big\|_2 ds + \int_0^t \big\| y(s) - y_n(s) \big\|_2 ds \\
&\leq \int_0^t M \big\| x(s) - x_n(s) \big\|_2 \, ds + \int_0^t \big\| y(s) - y_n(s) \big\|_2 ds
\end{aligned}$$

where $M > 0$ is the Lipschitz constant from f. It follows that

$$\begin{aligned}
\int_0^t M \big\| x(s) - x_n(s) \big\|_2 \, ds \;\; + \;\; & \int_0^t \big\| y(s) - y_n(s) \big\|_2 ds \\
& \leq TM \big\| x(s) - x_n(s) \big\|_2 + \int_0^t \big\| y(s) - y_n(s) \big\|_2 \, ds.
\end{aligned}$$

Thus,

$$\begin{aligned}
\|x - x_n\|_2 &\leq TM \left\| x(s) - x_n(s) \right\|_2 + \int_0^t \left\| y(s) - y_n(s) \right\|_2 ds \\
\implies \qquad \|x - x_n\|_2 \, (1 - TM) &\leq \int_0^t \left\| y(s) - y_n(s) \right\|_2 ds \\
\implies \qquad \|x - x_n\|_2 &\leq \frac{1}{(1 - TM)} \int_0^t \left\| y(s) - y_n(s) \right\|_2 ds.
\end{aligned}$$

Again, we have T, $M > 0$ and $\|y(s) - y_n(s)\|_2 \to 0$ and this completes the proof.

□

4.3 One-Dimensional Heat Equation

In this section, we will illustrate the new approach and theoretical results presented in Section 4.2 with a specific Volterra integro-differential equation in which the kernel generates a one dimensional heat equation.

Consider a Volterra integro-differential equation

$$\begin{aligned} \dot{x}(t) &= -x(t) + \int_0^t K(t-s)x(s)\,ds \\ x(0) &= 1 \end{aligned} \tag{4.13}$$

such that the transfer function is given by

$$g(s) = \frac{2\tanh(\frac{\sqrt{s}}{2})}{s\sqrt{s}},$$

where $g(s) = \mathcal{L}(K(t))$. Here $x \in L_2(0,T;\mathbb{R})$ and $K \in L_1 \cap L_2(0,T;\mathbb{R})$.

Theorem 4.6 *The transfer function*

$$g(s) = \frac{2\tanh(\frac{\sqrt{s}}{2})}{s\sqrt{s}}$$

for (4.13) *is realizable.*

Proof: For $s > 0$, let $\mathbb{R}$ be the input and output spaces; then for $u_1, u_2 \in \mathbb{R}$ we want to show $g(s) \in L(\mathbb{R},\mathbb{R})$.

$$\begin{aligned} g(s)(u_1+u_2) &= \frac{2\tanh(\frac{\sqrt{s}}{2})}{s\sqrt{s}}(u_1+u_2) \\ &= \frac{2\tanh(\frac{\sqrt{s}}{2})}{s\sqrt{s}}u_1 + \frac{2\tanh(\frac{\sqrt{s}}{2})}{s\sqrt{s}}u_2 \\ &= g(s)u_1 + g(s)u_2. \end{aligned}$$

Now for $u \in \mathbb{R}$ and $\alpha \in \mathbb{R}$,

$$\begin{aligned} g(s)\alpha u &= \frac{2\tanh(\frac{\sqrt{s}}{2})}{s\sqrt{s}}\alpha u \\ &= \alpha\frac{2\tanh(\frac{\sqrt{s}}{2})}{s\sqrt{s}}u \\ &= \alpha g(s)u. \end{aligned}$$

This implies $g(s) \in L(\mathbb{R}, \mathbb{R})$. To show g uniformly bounded on $L(\mathbb{R}, \mathbb{R})$, we fix $s = \beta > 0$ and consider

$$\begin{aligned}
\|g(s)\| &= \max_{u \in \mathbb{R}\setminus\{0\}} \frac{\|g(s)u\|_{\mathbb{R}}}{\|u\|_{\mathbb{R}}} \\
&= \max_{u \in \mathbb{R}\setminus\{0\}} \frac{\left\| \frac{2\tanh(\frac{\sqrt{s}}{2})}{s\sqrt{s}} u \right\|_{\mathbb{R}}}{\|u\|_{\mathbb{R}}} \\
&\leq \max_{u \in \mathbb{R}\setminus\{0\}} \frac{\left\| \frac{2\tanh(\frac{\sqrt{s}}{2})}{s\sqrt{s}} \right\|_{\mathbb{R}} \|u\|_{\mathbb{R}}}{\|u\|_{\mathbb{R}}} \\
&= \max_{u \in \mathbb{R}\setminus\{0\}} \left\| \frac{2\tanh(\frac{\sqrt{s}}{2})}{s\sqrt{s}} \right\|_{\mathbb{R}}.
\end{aligned}$$

Before we move on, we simplify $g(s)$ by

$$\begin{aligned}
\frac{2\tanh(\frac{\sqrt{s}}{2})}{s\sqrt{s}} &= \frac{2}{s\sqrt{s}} \frac{\sinh(\frac{\sqrt{s}}{2})}{\cosh(\frac{\sqrt{s}}{2})} \\
&= \frac{2}{s\sqrt{s}} \frac{e^{(\frac{\sqrt{s}}{2})} - e^{-(\frac{\sqrt{s}}{2})}}{2} \frac{2}{e^{(\frac{\sqrt{s}}{2})} + e^{-(\frac{\sqrt{s}}{2})}} \\
&= \frac{2}{s\sqrt{s}} \frac{e^{(\frac{\sqrt{s}}{2})} - e^{-(\frac{\sqrt{s}}{2})}}{e^{(\frac{\sqrt{s}}{2})} + e^{-(\frac{\sqrt{s}}{2})}} \\
&= \frac{2\left(\frac{e^{\frac{s}{4}} - 1}{e^{\frac{\sqrt{s}}{2}}} \right)}{s\sqrt{s}\left(\frac{e^{\frac{s}{4}} + 1}{e^{\frac{\sqrt{s}}{2}}} \right)} \\
&= \frac{2\big(e^{\frac{s}{4}} - 1\big)}{s\sqrt{s}\big(e^{\frac{s}{4}} + 1\big)} \\
&= \frac{2\big(e^{\frac{s}{4}} + 1\big)}{s\sqrt{s}\big(e^{\frac{s}{4}} + 1\big)} - \frac{4}{s\sqrt{s}\big(e^{\frac{s}{4}} + 1\big)} \\
&= \frac{2}{s\sqrt{s}} - \frac{4}{s\sqrt{s}\big(e^{\frac{s}{4}} + 1\big)}.
\end{aligned}$$

This implies

$$\begin{aligned}\|g(s)\| &\leq \frac{2}{s\sqrt{s}} - \frac{4}{s\sqrt{s}\big(e^{\frac{s}{4}}+1\big)} \\ &= \frac{2}{\beta\sqrt{\beta}} - \frac{4}{\beta\sqrt{\beta}\big(e^{\frac{\beta}{4}}+1\big)}.\end{aligned}$$

On the set $\{s \in \mathbb{C} |\ \text{Re}\ s > 0\}$, $g(s)$ is analytic and

$$g'(s) = \frac{e^{\frac{s}{4}}}{s^{\frac{3}{2}}(e^{\frac{s}{4}}+1)^2} + \frac{6}{s^{\frac{5}{2}}(e^{\frac{s}{4}}+1)} - \frac{3}{s^{\frac{5}{2}}}.$$

Now we want to look at the limit of $g(s)$, we consider

$$\begin{aligned}\lim_{x\to\infty} \max y\, \|g(x+iy)\| &= \lim_{x\to\infty} \max y \left| \frac{2}{(x+iy)\sqrt{x+iy}} - \frac{4}{(x+iy)\sqrt{x+iy}\big(e^{\frac{x+iy}{4}}+1\big)} \right| \\ &\leq \lim_{x\to\infty} \max y \left(\frac{2}{|(x+iy)|\,|\sqrt{x+iy}|} + \frac{4}{|(x+iy)||\sqrt{x+iy}||e^{\frac{x+iy}{4}}+1|} \right).\end{aligned}$$

Using the fact that

$$\sqrt{z} = \sqrt{r}e^{i\theta/2}$$

where $z = x+iy$, $r^2 = x^2+y^2$ and $\theta \in [0, 2\pi k]$, $k = 1, 2, ...$, we have

$$\begin{aligned}|\sqrt{z}| &= |\sqrt{r}|\,|e^{i\theta/2}| \\ &= |\sqrt{x^2+y^2}|, \qquad \text{since } |e^{i\theta/2}| = 1.\end{aligned}$$

It follows that the limit above is equal to zero. To see this, we note that

$$\begin{aligned}\lim_{x\to\infty} \max y\, \|g(x+iy)\| &\leq \lim_{x\to\infty} \max y \left(\frac{2}{\sqrt{x^2+y^2}\sqrt{x^2+y^2}} + \frac{4}{\sqrt{x^2+y^2}\sqrt{x^2+y^2}\,|\,e^{\frac{x+iy}{4}}+1|} \right) \\ &= \lim_{x\to\infty} \max y \left(\frac{2}{x^2+y^2} + \frac{4}{(x^2+y^2)\,|\,e^{\frac{x+iy}{4}}+1|} \right) \\ &= \lim_{x\to\infty} y \left(\frac{2}{x^2} + \frac{4}{x^2\,|\,e^{\frac{x}{4}}|\,|\,e^{\frac{iy}{4}}|} \right) \\ &= \lim_{x\to\infty} y \left(\frac{2}{x^2} + \frac{4}{x^2\,|\,e^{\frac{x}{4}}|} \right) \\ &= y \lim_{x\to\infty} \left(\frac{2}{x^2} + \frac{4}{x^2\,|\,e^{\frac{x}{4}}|} \right) \\ &= 0.\end{aligned}$$

An application of Theorem 1.4 completes the proof.

□

We now construct a state representation for the transfer function, $g(s)$, given above. Consider a controlled heat equation from [17]

$$\begin{aligned} \frac{\partial z}{\partial t}(u,t) &= \frac{\partial^2 z}{\partial u^2}(u,t) + b(u)x(t), \\ \frac{\partial z}{\partial u}(0,t) &= 0 = \frac{\partial z}{\partial u}(1,t), \qquad z(u,0) = z_0(u), \\ y(t) &= \int_0^1 c(u)z(u,t)du, \end{aligned} \tag{4.14}$$

where

$$\begin{aligned} b(u) &= 2 \cdot 1_{\left[\frac{1}{2},1\right]}(u) \\ c(u) &= 2 \cdot 1_{\left[0,\frac{1}{2}\right]}(u) \end{aligned}$$

with

$$1_{\left[\alpha,\beta\right]}(u) = \begin{cases} 1, & \alpha \le u \le \beta \\ 0, & otherwise. \end{cases}$$

Substitute for $c(u)$, we get

$$y(t) = 2\int_0^{\frac{1}{2}} z(u,t)du.$$

System (4.14) describes heat conduction in a metal rod of length one. We use an additional heating element around the point $u = \frac{3}{4}$. $z(u,t)$ represents the temperature of the rod at time t and position u and $z_0(u)$ is the initial temperature. We measure its temperature around the point $u = \frac{1}{4}$ and we also assume that there is no cooling or heating at either the end of the rod. The functions b and c represent the "shaping functions" around the control point $u = \frac{3}{4}$ and the sensing point $u = \frac{1}{4}$, respectively.

Suppose $\hat{z}(u,s)$ is the Laplace transform of $z(u,t)$ where s is the parameter. Now taking the Laplace transform of the PDE system (4.14) with respect

to t, we get the following boundary value problem for $\hat{z}(u,s)$

$$\begin{aligned} s\hat{z}(u,s) &= \frac{d^2\hat{z}}{du^2}(u,s) + 2\cdot 1_{\left[\frac{1}{2},1\right]}(u)\hat{x}(s), \\ \frac{d\hat{z}}{du}(0,s) &= 0 = \frac{d\hat{z}}{du}(1,s). \end{aligned} \tag{4.15}$$

Note that $z_0(u)$ is assumed to be 0 since the transfer functions consider zero initial state response. Also, we employ $\hat{x}(s)$ to be the Laplace transform of $x(t)$. It follows that system (4.15) can be written as a first order system below

$$\frac{d}{du}\begin{pmatrix} \hat{z} \\ \frac{d\hat{z}}{du} \end{pmatrix} = \begin{pmatrix} 0 & 1 \\ s & 0 \end{pmatrix}\begin{pmatrix} \hat{z} \\ \frac{d\hat{z}}{du} \end{pmatrix} - \begin{pmatrix} 0 \\ 2 \end{pmatrix} 1_{[\frac{1}{2},1]}\hat{x}(s).$$

For $s \neq 0$, the solution to the above system would be

$$\begin{pmatrix} \hat{z}(u,s) \\ \frac{d\hat{z}}{du}(u,s) \end{pmatrix} = \begin{pmatrix} \cosh(\sqrt{s}u) & \frac{1}{\sqrt{s}}\sinh(\sqrt{s}u) \\ \sqrt{s}\sinh(\sqrt{s}u) & \cosh(\sqrt{s}u) \end{pmatrix}\begin{pmatrix} \hat{z}(0,s) \\ 0 \end{pmatrix}$$

$$- 2\int_0^u \begin{pmatrix} \frac{1}{\sqrt{s}}\sinh(\sqrt{s}(u-\xi)) \\ \cosh(\sqrt{s}(u-\xi)) \end{pmatrix} 1_{[\frac{1}{2},1]}(\xi)\hat{x}(s)\, d\xi.$$

Also since we have

$$\begin{aligned} 0 &= \frac{d\hat{z}}{dx}(1,s) = \sqrt{s}\sinh(\sqrt{s})\hat{z}(0,s) - 2\int_{\frac{1}{2}}^1 \cosh(\sqrt{s}(1-\xi))\hat{x}(s)\, d\xi \\ &= \sqrt{s}\sinh(\sqrt{s})\hat{z}(0,s) + 2\left[\frac{1}{\sqrt{s}}\sinh(\sqrt{s}(1-\xi))\right]_{\frac{1}{2}}^1 \hat{x}(s) \\ &= \sqrt{s}\sinh(\sqrt{s})\hat{z}(0,s) - \frac{2}{\sqrt{s}}\sinh(\frac{\sqrt{s}}{2})\hat{x}(s), \end{aligned}$$

it follows that

$$\begin{aligned} \hat{z}(0,s) &= \frac{\frac{2}{\sqrt{s}}\sinh(\frac{\sqrt{s}}{2})\hat{x}(s)}{\sqrt{s}\sinh(\sqrt{s})} \\ &= \frac{2\sinh(\frac{\sqrt{s}}{2})\hat{x}(s)}{s\sinh(\sqrt{s})} \\ &= \frac{2\hat{x}(s)}{s}\left(\frac{e^{\frac{\sqrt{s}}{2}} - e^{-\frac{\sqrt{s}}{2}}}{e^{\sqrt{s}} - e^{-\sqrt{s}}}\right) \end{aligned}$$

$$\begin{aligned} &= \frac{2\hat{x}(s)}{s}\left(\frac{e^{\frac{\sqrt{s}}{2}}-e^{-\frac{\sqrt{s}}{2}}}{e^{\sqrt{s}}-e^{-\sqrt{s}}}\right)\left(\frac{e^{\frac{\sqrt{s}}{2}}+e^{-\frac{\sqrt{s}}{2}}}{e^{\frac{\sqrt{s}}{2}}+e^{-\frac{\sqrt{s}}{2}}}\right) \\ &= \frac{2\hat{x}(s)}{s(e^{\frac{\sqrt{s}}{2}}+e^{-\frac{\sqrt{s}}{2}})} \\ &= \frac{\hat{x}(s)}{s\cosh(\frac{\sqrt{s}}{2})}, \end{aligned}$$

and

$$\hat{z}(u,s) = \frac{\hat{x}(s)\cosh(\sqrt{s}u)}{s\cosh(\frac{\sqrt{s}}{2})} - \int_0^u \frac{\sinh(\sqrt{s}(u-\xi))1_{[\frac{1}{2},1]}(\xi)}{\sqrt{s}}\, d\xi\, \hat{x}(s).$$

We obtain $\hat{y}(s)$ as

$$\begin{aligned} \hat{y}(s) &= 2\int_0^{\frac{1}{2}} \hat{z}(u,s)du = 2\int_0^{\frac{1}{2}} \cosh(\sqrt{s}u)du\, \frac{\hat{x}(s)}{s\cosh(\frac{\sqrt{s}}{2})} \\ &\quad - 4\int_0^{\frac{1}{2}}\int_0^u \frac{\sinh(\sqrt{s}(u-\xi))1_{[\frac{1}{2},1]}(\xi)}{\sqrt{s}}\, d\xi\, \hat{x}(s)\, du. \end{aligned}$$

Since we integrate u from 0 to $\frac{1}{2}$ and $\xi \leq u$, the second integral vanishes by $1_{[\frac{1}{2},1]}(\xi)$. It follows that

$$\hat{y}(s) = \frac{2\sinh(\frac{\sqrt{s}}{2})}{s\sqrt{s}\cosh(\frac{\sqrt{s}}{2})}\hat{x}(s) - 0.$$

It follows from convolution theorem that

$$y(t) = \int_0^t K(t-s)x(s)ds$$

where

$$K(t-\alpha) = \left[\mathcal{L}^{-1}\left(\frac{2\tanh(\frac{\sqrt{s}}{2})}{s\sqrt{s}}\right)\right](t-\alpha)$$

and

$$x(t) = \left[\mathcal{L}^{-1}\hat{x}(s)\right](t).$$

Therefore, the Volterra integro-differential equation given in (4.13) can be written as an ODE coupled with a PDE below

$$\begin{aligned} \dot{x}(t) &= -x(t) + y(t) \\ z_t(u,t) &= z_{uu}(u,t) + 2 \cdot 1_{[\frac{1}{2},1]}(u)x(t) \\ \frac{\partial z}{\partial x}(0,t) &= 0 = \frac{\partial z}{\partial x}(1,t), \qquad z(u,0) = z_0(u), \\ y(t) &= 2\int_0^{\frac{1}{2}} z(u,t)\,du \\ x(0) &= 1. \end{aligned} \tag{4.16}$$

From the proof in Theorem 4.6 above and Definition 4.5,

$$g(s) = \frac{2\tanh(\frac{\sqrt{s}}{2})}{s\sqrt{s}}$$

is the transfer function of PDE system (4.14).

Now we want consider the heat equation (4.14) and define the state space, X, to be $X = L_2(0,1)$. We let A be defined by

$$Az = \frac{d^2z}{du^2}$$

with

$$\begin{aligned} D(A) = \; & \{z \in L_2(0,1) \,|\, z, \tfrac{dz}{du} \text{ are absolutely continuous,} \\ & \tfrac{d^2z}{du^2} \in L_2(0,1) \text{ and } \tfrac{dz}{du}(0) = 0 = \tfrac{dz}{du}(1)\}. \end{aligned}$$

Then it is well known that A is closed and the eigenvalues of A are $\lambda_n = -n^2\pi^2$, $n \geq 0$, which with the correponding eigenvectors $\phi_n(x) = \sqrt{2}\cos(n\pi x)$ for $n \geq 1$, $\phi_0 = 1$, form an orthornormal basis for $L_2(0,1)$. Here A is the Riesz-spectral operator given by

$$Az = \sum_{n=0}^{\infty} -n^2\pi^2\langle z, \phi_n\rangle\phi_n \qquad \text{for } z \in D(A),$$

where

$$D(A) = \{z \in L_2(0,1) \,|\, \sum_{n=1}^{\infty} n^4\pi^4|\langle z, \phi_n\rangle|^2 < \infty\}.$$

Also, the operators $B \in L_2(0,1)$ and $C \in D(A)$ are defined to be

$$B\phi = 2 \cdot 1_{[\frac{1}{2},1]}(u)\phi$$

and

$$C\theta = 2 \int_0^{\frac{1}{2}} \theta(u)\, du$$

repectively. Then, by Theorem 4.4, the transfer function $G(s)$ of the heat equation in (4.14) is given by

$$\begin{aligned} G(s) &= \frac{1}{s} - \sum_{n=1}^{\infty} \frac{8\sin^2(\frac{n\pi}{2})}{(s+(n\pi)^2)(n\pi)^2} \\ &= \frac{1}{s} - \sum_{r=0}^{\infty} \frac{8}{(s+(2r+1)^2\pi^2)(2r+1)^2\pi^2} \end{aligned}$$

and see [17] for details. Since the transfer function is unique, $g(s)$, can also be represented as an infinite series

$$g(s) = \frac{2\tanh(\frac{\sqrt{s}}{2})}{s\sqrt{s}} = \frac{1}{s} - \sum_{r=0}^{\infty} \frac{8}{(s+(2r+1)^2\pi^2)(2r+1)^2\pi^2}.$$

Following the ideas from Section 4.2, we truncate the infinite series above at N and then construct A_N, B_N, and C_N from the truncated series $g_N(s)$. From there, we derive an ODE system below to approximate the given Volterra integro-differential equation (4.13)

$$\begin{aligned} \dot{x}(t) &= -x(t) + C_N z_N(t) \\ \dot{z}_N(t) &= A_N z_N(t) + B_N x(t) \\ x(0) &= 1, \qquad\qquad z_N(0) = 0. \end{aligned} \tag{4.17}$$

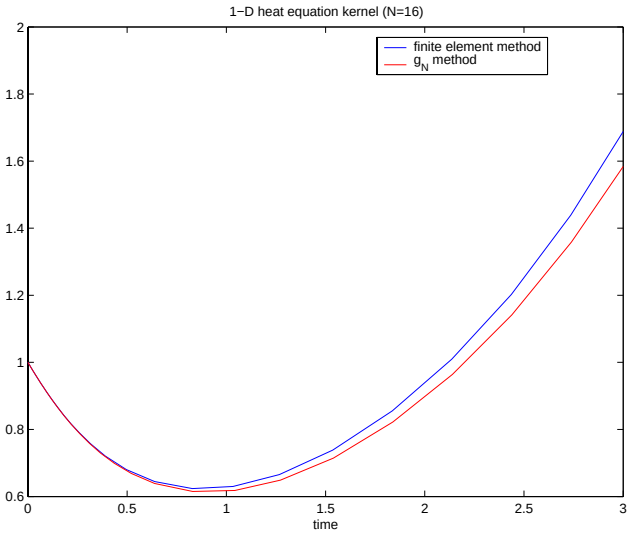

Figure 4.1: Kernel for the 1-D Heat Equation with Neumann boundary condition (N=16).

We compare our numerical results against the solutions from a finite element code with N being the number of elements. With the finite element method, we approximate the heat equation and then construct the approximate operators A_N, B_N and C_N. Again, we can write the approximate A_N, B_N, and C_N, which are standard from the finite element method, to contruct ODE system (4.17) above. Figure 4.1 provides the solution of system (4.16) using the finite element method and the truncated method on the transfer function. $N = 16$ is used for both methods and it is obvious that the solutions are very close to each other.

It is well known that the heat equation with Neumann boundary conditions is a stable problem and the finite element methods provide convergent solutions to the exact solution of the heat equation. It follows that solving system (4.16) with the idea of truncating the transfer function's series at N gives very precise results with sufficiently large N. Figure 4.2 and 4.3 also provide numerical results of system (4.16) from the two methods mentioned with $N = 32$ and $N = 64$ respectively. It is noticeable that as N gets large, the two approximations are very close. The approximate ODE system (4.17) generated from both methods is solved by MATLAB function *ode*23*s*, the solutions are plotted in Figure 4.1, 4.2, 4.3, and the computing times are

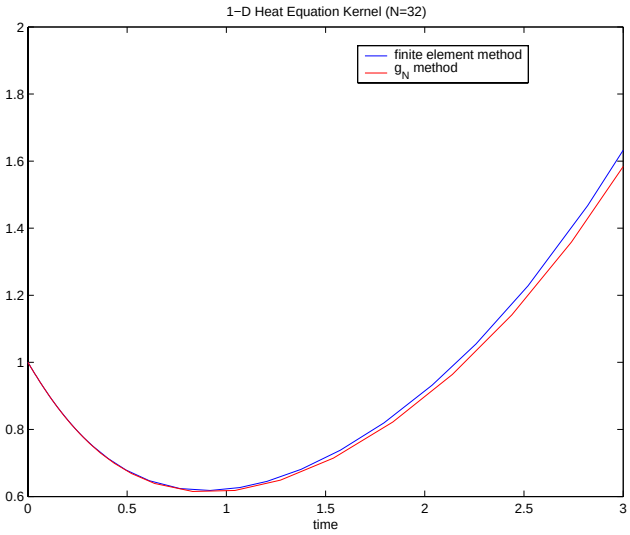

Figure 4.2: Kernel for the 1-D Heat Equation with Neumann boundary condition (N=32).

listed in Table 4.1. The computing times of the two methods with different N values in Table 4.1 suggest that the truncated series method is more efficient time-wise than the finite element method. Moreover, when using MATLAB function *ode*45 to solve for system (4.17), the truncated method is a lot slower than our finite element method. In fact, with $N = 64$, we were not able to solve system (4.17) using the truncated series method with *ode*45. It makes sense that MATLAB function *ode*23*s* is more efficient than *ode*45 when solving the approximated system (4.17) by truncating series g_N method because the eigenvalues of A, λ_n, gets closer to 0 as N gets large. In addition, even with our finite element method, using MATLAB function *ode*23*s* to solve for system (4.17) is faster than using function *ode*45.

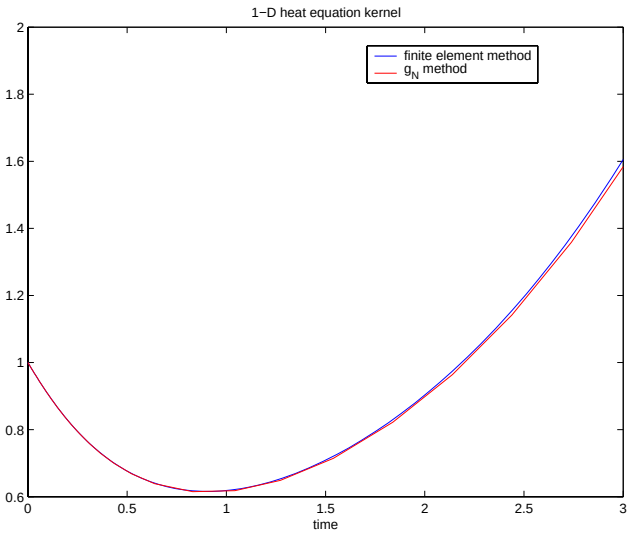

Figure 4.3: Kernel for the 1-D Heat Equation with Neumann boundary condition (N=64).

N	Truncated Series Method	Finite Element Method
16	0.4000	0.6510
32	0.5610	2.6440
64	0.8110	30.9050

Table 4.1: Computing time of finite element method and truncated series method in seconds.

Chapter 5

Conclusions and Future Work

It is obvious that the internal state method is more efficient than the direct numerical method in all the cases presented in this paper. This agrees with the findings of other authors relative to electromagnetic systems [see 3]. In addition, there is a direct correlation between the internal state method and the realization theory since the kernel $K(t)$ needs to have state representations for the internal state method to be applicable. In general, when the Laplace transfrom of $K(t)$, $\hat{K}(s)$, is a uniformly bounded $L(U,Y)$-valued function that is analytic on the right half plane with a limit in the positive direction, then $K(t)$ can be represented by a linear system. Once a kernel is verified to be realizable, the next complication is to construct the realization that corresponds to the kernel. This task can get very complicated at times, such as the one-dimensional heat equation in Section 4.3. If we were given a Volterra integro-differential equation with such a transfer function, it would probably take us a long time to construct the controlled heat equation in Section 4.3 to apply the internal state method. Therefore, the results in Section 4.2 are very beneficial since we can avoid the state representation formation problem. So far, we have only studied our new approach of approximating a Volterra integro-differential equation for the case where $K(t)$ is of nuclear type. We are planning to extend our study to the case where $K(t)$ is not nuclear. Also, the input and output operators, B and C, respectively, are considered to be bounded for the results in Section 4.2; hence, we would like to investigate if similar results would hold for unbounded B and C. We shall also apply our techniques to kernels that are not realizable as defined in the presentation. We believe this approach for approximating solutions of Volterra integro-differential equations has great potential since not only

does it help us to avoid the realization construction problem, it is faster in computing time when compared to some numerical methods for solving complicated PDE systems. When compared to the direct numerical method, we believe that our scheme will allow us to avoid the usual problems of weakly singular kernels.

Most of the problems in this paper consider state representations of the kernels to be time-invariant linear systems. However, there is one problem in Chapter 3, that is problem of Section 3.6, the corresponding realization of a given kernel is a time-variant linear system. As shown in that problem, the internal state idea out-performs the direct numerical approach. Therefore, it is worthwhile to do more research in realization theory on time-variant systems. As far as we know, there is only one theoretical result on time-variant systems in realization theory in [22]. This is a research area we also wish to pursue.

Bibliography

[1] A. Ackleh, H.T. Banks, and G.A. Pinter. Well-posedness results for models of elastomers. *CRSC Technical Report CRSC-TR00-21, N. C. State Univ.,* September 2000.

[2] H.T. Banks, D.M. Bortz and S.E. Holte. Incorporation of variability into the modeling of viral delays in HIV infection dynamics. *Mathematical Biosciences*, 183:63-91, 2003.

[3] H.T. Banks, M.W. Buksas and T. Lin. Electromagnetic material interrogation using conductive interfaces and acoustic wavefronts. *SIAM Frontiers in Applied Mathematics*. SIAM, Philadelphia, 2000.

[4] H.T. Banks and J.A. Burns. Hereditary Control Problems: Numerical methods based on averaging approximations. *SIAM J. Contr. Opt.,* 16(2):169-208, 1978.

[5] H.T. Banks and F. Kappel. Spline approximations for functional differential equations. *J. Diff. Eqs*, 34:496-522, 1979.

[6] H.T. Banks, N.G. Medhin and G.A. Pinter. Multiscale considerations in modeling of nonlinear elastomers. *CRSC Technical Report CRSC-TR03-42, N. C. State Univ.,* October 2003; *J. Comp. Meth. Sci. and Engr.,* to appear.

[7] H.T. Banks and G.A. Pinter. Damping: Hysteretic damping and models. *Encyclopedia of Vibration (S.G Braun, et. al., eds)*. Academic Press, London, 658-664, 2001.

[8] H.T. Banks and G.A. Pinter. A probabilistic multiscale approach to hysteresis in shear wave propagation in biotissue. *CRSC Technical Report*

CRSC-TR04-03, N. C. State Univ., January 2004; *Multiscale Modeling and Simulation,* submitted.

[9] H.T. Banks, G.A. Pinter and L.K. Potter. Modeling of nonlinear hysteresis in elastomers under uniaxial tension. *J. Intelligent Mat. Systems and Structures*, 10:116-134, 1999.

[10] H.T. Banks, I.G. Rosen, and K. Ito. A Spline Based Technique for Computing Riccati Operators and Feedback Controls in Regulator Problems for Delay Equations. *SIAM J. Sci. Stat. Comput.*, 5:830-855, 1984.

[11] J.S. Baras and R.W. Brockett. H^2-Functions and infinite-dimensional Realization Theory. *SIAM J. Control*, 13:221-241, 1975.

[12] H. Brunner and P.J. van der Houwen. *The numerical solution of Volterra equations*. Elsevier Science Publishing Company Inc., New York, 1986.

[13] J.A. Burns, E.M. Cliff and T.L. Herdman. A state-space model for an aero-elastic system. *22nd IEEE Conference on Decision and Control*, 3:1074-1077, 1983.

[14] J.A. Burns, K. Ito, and G. Propst. On NonConvergence of Adjoint Semigroups for Control Systems with Delays. *SIAM J. Contr. Opt.,* 26:1442-1454, 1988.

[15] E.M. Cliff and J.A. Burns. Euclidean Controllable Realizations of Linear Hereditary Systems. *Mathematical Sytems Theory,* 12:133-149, 1978.

[16] R.V. Culshaw, S. Ruan, and G. Webb. A mathematical model of cell-to-cell spread of HIV-1 that includes a time delay. *J. Math.Biol.*, 46:425-444, 2003.

[17] R.F Curtain and H.J. Zwart. *An Introduction to Infinite-Dimensional Linear Systems Theory.* Springer-Verlag, New York, 1995.

[18] R.D. Driver. *Ordinary and Delay Differential Equations*. Springer- Verlag, New York, 1977.

[19] Y.C. Fung. *Biomechanics: Mechanical properties of living tissues*. Springer-Verlag, New York, 1993.

[20] K. Glover, R.F. Curtain, and J.R. Partington. Realisation and approximation of linear infinite-dimensional systems with error bounds. *SIAM J. Contr. Opt.*, 26(4):863-898, 1988.

[21] J.W. Helton. Systems with Infinite-Dimensional State Space: The Hilbert Space Approach. *Proceedings of the IEEE*, 64:145-160, 1976.

[22] T. Kailath. *Linear Systems.* Prentice-Hall, Inc., New Jersey, 1980.

[23] G.S.K. Wolkowicz, H. Xia and S. Ruan. Competition in the chemostat: A distributed delay model and its global asymptotic behavior. *SIAM J. Appl. Math.*, 57:1281-1310, 1997.

[24] L.A. Zadeh and C.A. Desoer. *Linear System Theory: The State Space Approach.* McGraw-Hill Book Company, New York, 1963.

Vita

Hoan Kim Huynh Nguyen was born to Phu Nguyen and Nhieu Huynh on November 2^{nd}, 1978 in Saigon, Vietnam. Hoan and her younger brother, Vu, spent part of their childhood in Vietnam and part of it in Alexandria, Virginia. In 1997, she graduated with honors from Annandale High School and came to Virginia Tech with a T.W. Hatcher Scholarship. During her undergraduate career at Virginia Tech, she received the David P. Roselle Scholarship and the Senior Award. She graduated in December 1999 with a Commonwealth Scholar Honor Diploma and a minor in Chemistry. In June 2000, she joined Naval Research Laboratory working on developing algorithms to track radar signals while continuing her graduate study at an extended campus of Virginia Tech in Northern Virginia. In December 2000, she received her Master's degree in Mathematics. The following fall, Hoan returned to Virginia Tech as a full-time doctoral student under the supervision of Professor Terry L. Herdman. She is expected to graduate with a Doctoral Degree in May 2004 and then join Statistical and Applied Mathematical Sciences Institute (SAMSI) as a postdoctoral fellow in the fall of 2004.